PCCP

ROYAL SOCIETY OF CHEMISTRY

PERSPECTIVE

View Article Online
View Journal | View Issue

Cite this: *Phys. Chem. Chem. Phys.*, 2021, **23**, 24080

Strategies used by nature to fix the red, purple and blue colours in plants: a physical chemistry approach

Nuno Basílio, *[a] Johan Mendoza, [a] André Seco, [a] Joana Oliveira, [b] Victor de Freitas [b] and Fernando Pina *[a]

While identified by the respective flavylium cation, anthocyanins are much more than this molecule. The flavylium cation (generally appearing only at very acidic pH values) is one of the molecules of a complex sequence of pH dependent molecular species reversibly interconnected by different chemical reactions. These species include the red flavylium cation, purple quinoidal base and blue or bluish anionic quinoidal bases. At the common pH of the vacuoles of simpler anthocyanins, the red flavylium cation is present only at very acidic pH values and at moderately acidic pHs there is no significant colour of the purple quinoidal base. Moreover, the blue or bluish anionic quinoidal base appearing around neutral pH values is not stable. Intermolecular (copigmentation) and intramolecular (in acylated anthocyanins) interactions increase the colour hue and yield bathochromic shifts in the absorption bands, permitting to extend the pH domain of the flavylium cation and increase the mole fraction of the quinoidal bases. Metal complexation is another strategy. In particular, the Al^{3+} cation plays an essential role in the blue colour of hydrangea. The most sophisticated structures are however the metaloanthocyanins, such as the one that gives the blue colour of *commelina communis*, constituted of six anthocyanins, six flavanones and two metals. In this work we discuss how physical chemical tools are indispensable to account for the chemical behaviour of these complex systems. The experimental procedures and the equations needed to calculate all equilibrium constants of anthocyanins and the consequent pH dependent mole fraction distributions in the absence or presence of copigments are described in detail. Reverse pH jumps monitored by stopped flow have been shown to be an indispensable tool to calculate these parameters.

Received 3rd July 2021,
Accepted 28th September 2021

DOI: 10.1039/d1cp03034e

rsc.li/pccp

1. Introduction

Anthocyanins are responsible for a diversity of colours in plants, from orange-red to purple-blue hues. Moreover, they behave as photoprotective agents by absorbing excess visible and UV light,[1,2] giving protection to biotic and abiotic stresses,[3,4] play a role in plant reproduction attracting pollinators and seed dispersers by presenting attractive colors,[5,6] maintain the integrity of membranes in fruits and vegetables during the postharvest period, decelerating cell senescence,[7,8] and present numerous beneficial health effects owing to the multiple biological properties of these compounds (*e.g.*, antiproliferative, anti-inflammatory, and antimicrobial properties).[9,10]

The basic structure of anthocyanins is presented in Scheme 1.

In nature a variety of sugars can be attached in position 3 and 5, and seldom in other positions, like position 7. Nowadays, more than 700 related chemical structures have been identified in nature.[12] While usually represented by the coloured flavylium cation, this species is only stable under very acidic conditions (pH < 1), being reversibly transformed into a mixture of quinoidal bases, hemiketal and chalcones (see below for a more detailed discussion of these phenomena) under higher pH conditions. In simple but very common anthocyanins, such as mono and diglucoside anthocyanins, the colourless species (hemiketal and chalcones) are the major forms found in *in vitro* solutions of these dyes under slightly acidic and neutral conditions. It is therefore straightforward to conclude that, by themselves, these anthocyanins are not able to confer the colours observed in plants and that interactions with other (macro)molecular or ionic species

[a] *LAQV – REQUIMTE, Departamento de Química, Faculdade de Ciências e Tecnologia, Universidade Nova de Lisboa, 2829-516 Caparica, Portugal. E-mail: fp@fc.up.pt, nuno.basilio@fct.unl.pt, johanmen2a@gmail.com, am.seco@campus.fct.unl.pt*

[b] *LAQV – REQUIMTE, Departamento de Química e Bioquímica, Faculdade de Ciências, Universidade do Porto, Rua do Campo Alegre, 687, 4169-007 Porto, Portugal. E-mail: jsoliveira@fc.up.pt, vfreitas@fc.up.pt*

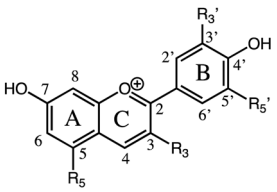

Pelargonidin ($R_{3'}$=H; $R_{5'}$=H; R_5=OH)
Peonidin ($R_{3'}$=OMe; $R_{5'}$=H; R_5=OH)
Cyanidin ($R_{3'}$=OH; $R_{5'}$=H; R_5=OH)
Malvidin ($R_{3'}$=OMe; $R_{5'}$=OMe; R_5=OH)
Petunidin ($R_{3'}$=OMe; $R_{5'}$=OH; R_5=OH)
Delphinidin ($R_{3'}$=OH; $R_{5'}$=OH; R_5=OH)

Scheme 1 Basic structure of anthocyanins and related compounds; R_3═R_5═OH, anthocyanidins; R_3═OGly; R_5═OH, monoglycosides; R_3═OGly; R_5═OGly, diglycosides; R_3═H, R_5═OGly, 3-deoxyanthocyanins; R_3═H, R_5═OH, 3-deoxyanthocyanidins; OGly = glycoside. Different monosaccharides (*e.g.*, glucose, galactose, rhamnose, and arabinose) and disaccharides (*e.g.*, rutinose, sambubiose, and sophorose) can be attached to the flavylium core, and these sugars can also be acylated with cinnamic acids (*e.g.*, caffeic, coumaric, ferrulic, and sinapic acids) or aliphatic acids (*e.g.*, acetic, malic, oxalic, and succinic acids).[11]

in complex natural matrixes must play an important role in colour stabilization and modulation. The strategies used by nature to overcome this drawback and the physical chemistry that is behind them are the main topic of this work.

Despite possessing relatively simple molecular structures, anthocyanins gave rise to very complex systems, exhibiting at least thirteen species in equilibrium (see Scheme 2). However, this complexity can be dramatically simplified since the flavylium cation behaves as a polyprotic acid. This property is used through this work to rationalize the experimental data. Three appendixes are included demonstrating mathematically this anthocyanin behaviour, which is also observed in the case of co-pigmentation and complexation with metals.

2. Anthocyanins are more than the flavylium cation[13]

Anthocyanins are identified by the respective flavylium cation as in Scheme 1. This fact could give rise to some misunderstandings, because the flavylium cation is only one of the numerous chemical species that are reversibly interconnected by external stimuli such as pH modifications, light and heat, from here on designated the multistate, Scheme 2.

At very acidic pH values generally pH $\leq$ 1 the flavylium cation is the sole observed species. However, upon addition of a base to the solutions at pH $\leq$ 1 (direct pH jumps) a sequence of chemical reactions takes place in acidic to moderately acidic solutions, as shown in Scheme 2 and eqn (1)–(4),

$$AH^+ + H_2O \underset{k_{-a}}{\overset{k_a}{\rightleftharpoons}} A + H_3O^+ \quad K_a \text{ proton transfer} \qquad (1)$$

$$AH^+ + 2H_2O \underset{k_{-h}}{\overset{k_h}{\rightleftharpoons}} B + H_3O^+ \quad K_h \text{ hydration} \qquad (2)$$

$$B \underset{k_{-t}}{\overset{k_t}{\rightleftharpoons}} Cc \quad K_t \text{ tautomerization} \qquad (3)$$

$$Cc \underset{k_{-i}}{\overset{k_i}{\rightleftharpoons}} Ct \quad K_i \text{ isomerization} \qquad (4)$$

Carrying out a mass balance of these species and representing in terms of AH^+ by means of eqn (1) to eqn (4), the pH dependent mole fraction distribution (χ) of these species can be calculated.

$$\chi_{AH^+} = \frac{[H^+]}{[H^+] + K_a'}; \qquad \chi_A + \chi_B + \chi_{Cc} + \chi_{Ct} = \chi_{CB} = \frac{K_a'}{[H^+] + K_a'} \qquad (5)$$

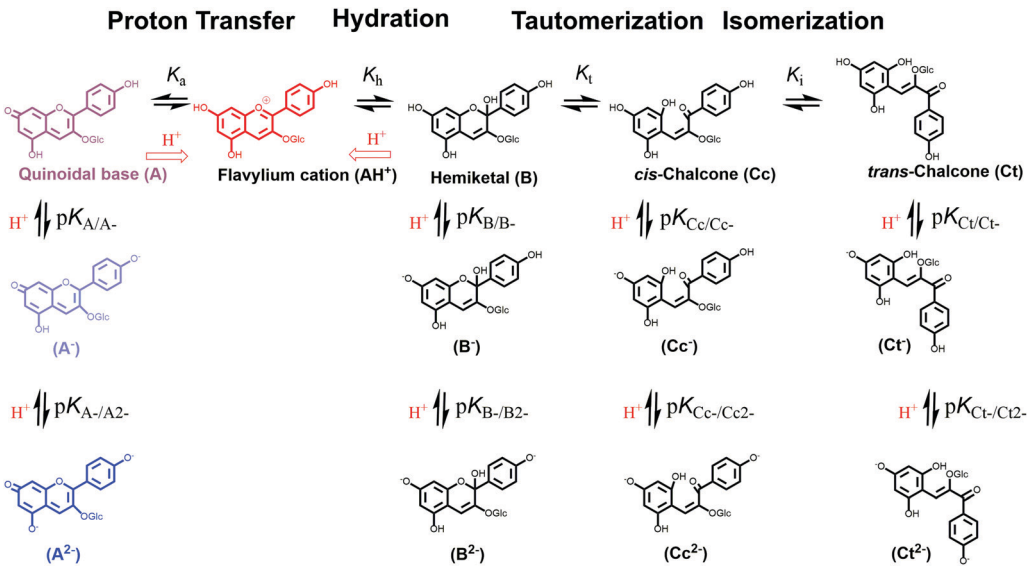

Scheme 2 Multistate of chemical species of cyanidin-3-glucoside in acidic to neutral aqueous solutions. $K_x = k_x/k_{-x}$ (x = a, h, t).

defining

$$K_a' = K_a + K_h + K_h K_t + K_h K_t K_i \quad (6)$$

with

$$CB = [A] + [B] + [Cc] + [Ct] \quad (7)$$

Inspection of eqn (5)–(7) allows for concluding that the complex system constituted of eqn (1)–(4) is reduced to a single acid base equilibrium involving the flavylium cation AH^+ and its conjugated base CB.

$$AH^+ + H_2O \rightleftharpoons CB + H_3O^+$$
$$K_a' = \frac{[CB][H^+]}{[AH^+]} \text{ global equilibrium} \quad (8)$$

At higher pH values anionic species are formed due to the deprotonation of the hydroxyl substituents. We consider only the first deprotonation because these are essentially the species that we have to deal with in this work, for example, in acylated anthocyanins.

$$A + H_2O \rightleftharpoons A^- + H_3O^+ \quad K_{A/A^-} \quad (9)$$

$$B + H_2O \rightleftharpoons B^- + H_3O^+ \quad K_{B/B^-} \quad (10)$$

$$Cc + H_2O \rightleftharpoons Cc^- + H_3O^+ \quad K_{Cc/Cc^-} \quad (11)$$

$$Ct + H_2O \rightleftharpoons Ct^- + H_3O^+ \quad K_{Ct/Ct^-} \quad (12)$$

A similar simplification can be done, eqn (13)

$$CB + H_2O \rightleftharpoons CB^- + H_3O^+ \quad K_a'' \text{ global equilibrium} \quad (13)$$

From eqn (13) and substituting the species of CB and CB^- in terms of AH^+, the following relation is obtained, eqn (14)

$$K_a'' = \frac{K_{A/A^-}K_a + K_{B/B^-}K_h + K_{Cc/Cc^-}K_h K_i + K_{Ct/Ct^-}K_h K_t K_i}{K_a'} \quad (14)$$

The fact that this complex system can be simplified considering AH^+ in equilibrium with its conjugated forms CB and CB^- is a breakthrough that allows for the simplification of the mathematical treatment. Both pK_a' and pK_a'' can be experimentally obtained similarly to a simple diprotic acid corresponding to the pH of two inflection points when the absorbance is represented as a function of pH.

If the equilibrium constants are known, it is straightforward to calculate the mole fractions of all species considering that the flavylium cation is a diprotic acid. See Appendix 1 for more details.

$$\chi_{AH^+} = \frac{[H^+]^2}{D}; \quad \chi_A = \frac{K_a[H^+]}{D}; \quad \chi_B = \frac{K_h[H^+]}{D}$$
$$\chi_{Cc} = \frac{K_h K_t[H^+]}{D}; \quad \chi_{Ct} = \frac{K_h K_t K_i[H^+]}{D}$$

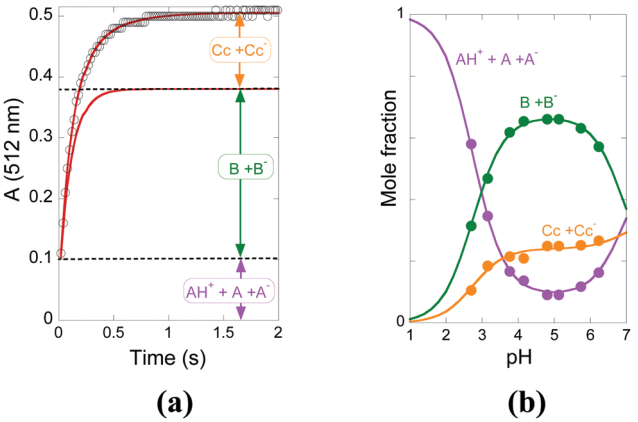

Fig. 1 (a) Kinetic trace obtained by stopped flow upon a reverse pH jump from equilibrated solutions of kuromanin at pH = 5.1 to pH = 1.0. The graph shows the three observed amplitudes and their assignment. (b) Mole fraction distribution at the pseudo-equilibrium.

And for the anionic species

$$\chi_{A^-} = \frac{K_{A/A^-}K_a}{D}; \quad \chi_{B^-} = \frac{K_{B/B^-}K_h}{D}; \quad \chi_{Cc^-} = \frac{K_{Cc/Cc^-}K_h K_t}{D};$$
$$\chi_{Ct^-} = \frac{K_{Ct/Ct^-}K_h K_t K_i}{D}$$

$$D = [H^+]^2 + K_a'[H^+] + K_a'K_a'' \quad (15)$$

In anthocyanins and many other flavylium derived multistates of species the isomerization is by far the slowest process of the kinetics and a pseudo-equilibrium can be defined as a transient state obtained before significant formation of *trans*-chalcone, eqn (1)–(3) and (5)–(7), and the respective pseudo-equilibrium constants are defined by eqn (16)–(19).

$$AH^+ + H_2O \rightleftharpoons CB^\wedge + H_3O^+ \quad K^\wedge_a \quad (16)$$

$$CB^\wedge = [A] + [B] + [Cc] \quad (17)$$

$$CB^\wedge + H_2O \rightleftharpoons CB^{\wedge -} + H_3O^+ \quad K^{\wedge\wedge}_a \quad (18)$$

$$CB^{\wedge -} = [A^-] + [B^-] + [Cc^-] \quad (19)$$

The mole fractions of the species at the pseudo equilibrium use the same set of equations as the equilibrium removing the contributions of *trans*-chalcone and substituting D in eqn (15) by $D^\wedge$ in eqn (20).

$$D^\wedge = [H^+]^2 + K^\wedge_a[H^+] + K^\wedge_a K^{\wedge\wedge}_a \quad (20)$$

3. How to calculate all equilibrium constants. Reverse pH jumps: a new paradigm

3.1. Stopped flow measurements

The most accurate method to achieve the equilibrium constants of the system is based on reverse pH jumps (defined by

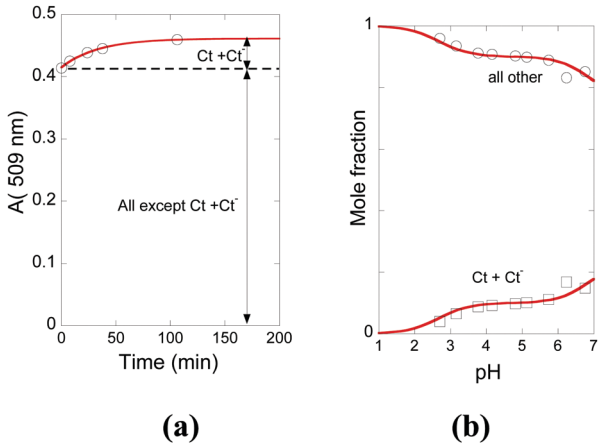

Fig. 2 (a) Kinetic trace obtained by a standard spectrophotomter upon a reverse pH jump from equilibrated solutions of kuromanin at pH = 5.1 to pH = 1.0. (b) Mole fraction distribution of *trans*-chalcone at the equilibrium.

the addition of acid back to pH $\leq$ 1 of equilibrated or pseud-equilibrated solutions at higher pH values)[14] monitored by stopped flow.[15] In Fig. 1a the trace of a typical reverse pH jump is shown. Three amplitudes are observed. The first is due to the flavylium cation absorption resulting from the conversion of all quinoidal bases (neutral and anionic) during the mixing time of the stopped flow together with some flavylium that, depending on the pH, can be at the equilibrium prior to the pH jump for lower pH values. The amplitude of the faster kinetic step results from the conversion of hemiketal into the flavylium cation, because at pH $\leq$ 1 the hydration/dehydration is faster than the tautomerization, due to the change of the kinetic regime.[14,16] Finally the last amplitude corresponds to the formation of more flavylium cations from *cis*-chalcone *via* hemiketal. Normalization of these amplitudes to unity gives directly the mole fraction distribution of the three species at the pseudo-equilibrium as shown in Fig. 1b.

3.2. Reverse pH jumps at longer timescales

The mole fractions of Ct + Ct^- can be calculated by following the reverse pH jump through a standard spectrophotometer, as shown in Fig. 2a. Extending to a series of pH jumps, the mole fraction distribution of Ct and its anionic form are calculated, Fig. 2b, and the mole fractions of AH^+, A + A^-, B + B^- and Cc + Cc^- are recalculated for the equilibrium, discounting those of Ct and Ct^-, Fig. 3. In Table 1 the equilibrium constants of cyanidin-3-*O*-glucoside (kuromanin) are shown. It should be emphasized that the constants regarding the anionic species have a higher uncertainty because of the propagation of errors law (they depend on the equilibrium constants of the neutral species) and due to the instability of the simpler anthocyanins at higher pH values, affecting more particularly the determination of the mole fractions of Ct.

4. How to simplify the complexity

Considering that in the stopped flow measurements $CB^{\wedge}$ and $CB^{-\wedge}$ are decomposed in terms of their components quinoidal bases, hemiketals and *cis*-chalcones, neutral and anionic,[15] the mole fraction of the three amplitudes of the stopped flow data can be written as in eqn (21)–(23)

$$\chi_{AH^+} + \chi_A + \chi_{A^-} = \frac{[H^+]^2 + a_0 K^{\wedge}_a [H^+] + a_1 K^{\wedge}_a K^{\wedge\wedge}_a}{D^{\wedge}} \quad (21)$$

where a_0 and a_1 are the parameters to adjust the respective curve in Fig. 1b.

Identically for the hemiketal and *cis*-chalcone

$$\chi_B + \chi_{B^-} = \frac{b_0 K^{\wedge}_a [H^+] + b_1 K^{\wedge}_a K^{\wedge\wedge}_a}{D^{\wedge}} \quad (22)$$

$$\chi_{Cc} + \chi_{Cc^-} = \frac{c_0 K^{\wedge}_a [H^+] + c_1 K^{\wedge}_a K^{\wedge\wedge}_a}{D^{\wedge}} \quad (23)$$

with $D^{\wedge}$ defined by eqn (20).

The fittings adjust the parameters a_n, b_n and c_n (n = 0, 1) and $K^{\wedge}_a$ and $K^{\wedge\wedge}_a$. These last two constants should be equal within the experimental error to those calculated from the two inflection points of the absorbance *versus* pH at the pseudo-equilibrium.

On the other hand, these mole factions can be written in terms of the respective equilibrium constants, removing the Ct contribution in the mole fractions of eqn (15).

$$\chi_{AH^+} + \chi_A + \chi_{A^-} = \frac{[H^+]^2 + K_a [H^+] + K_{A/A^-} K_a}{D^{\wedge}} \quad (24)$$

$$\chi_B + \chi_{B^-} = \frac{K_h [H^+] + K_{B/B^-} K_h}{D^{\wedge}} \quad (25)$$

$$\chi_{Cc} + \chi_{Cc^-} = \frac{K_h K_t [H^+] + K_{Cc/Cc^-} K_h K_t}{D^{\wedge}} \quad (26)$$

Comparing eqn (21) with eqn (24), eqn (22) with eqn (25) and (23) with eqn (26) the following important relations are obtained:

Table 1 Equilibrium constants of kuromain. Estimated error 5%

$pK^{\wedge}_a$	$pK^{\wedge\wedge}_a$	pK'_a	pK''_a	pK_a	K_h/M	K_t	K_i
2.75	6.95	2.7	6.9	3.8	1.2×10^{-3}	0.36	0.49

pK_{A/A^-}[a]	pK_{B/B^-}[a]	pK_{Cc/Cc^-}[a]	pK_{Ct/Ct^-}[a]
6.15	7.8	6.8	6.5

[a] Estimated error 10%.

For the neutral species

$$K_a = a_0 K^{\wedge}_a; \quad K_h = b_0 K^{\wedge}_a; \quad K_h K_t = c_0 K^{\wedge}_a \tag{27}$$

For the anionic species

$$K_{A/A^-} = \frac{a_1 K^{\wedge}_a K^{\wedge\wedge}_a}{K_a}; \quad K_{B/B^-} = \frac{b_1 K^{\wedge}_a K^{\wedge\wedge}_a}{K_h}; \quad K_{Cc/Cc^-} = \frac{c_1 K^{\wedge}_a K^{\wedge\wedge}_a}{K_h K_t} \tag{28}$$

These equations allow for calculation of all equilibrium constants involving AH^+, A, B and Cc. See Appendix 1 for more details.

The reverse pH jumps monitored using a standard spectrophotometer, as in Fig. 2b, give the mole fraction distribution of Ct and Ct^-. Similarly, the mole fractions of Fig. 2a can be expressed in terms of the parameters d_0 and d_1, eqn (29), or as in eqn (30).

$$\chi_{Ct} + \chi_{Ct^-} = \frac{d_0 K'_a [H^+] + d_1 K'_a K''_a}{D} \tag{29}$$

$$\chi_{Ct} + \chi_{Ct^-} = \frac{K_h K_t K_i [H^+] + K_{Ct/Ct^-} K_h K_t K_i}{D} \tag{30}$$

Comparing eqn (29) with eqn (30)

$$K_i = \frac{d_0 K'_a}{K_h K_t}; \quad K_{Ct/Ct^-} = \frac{d_1 K'_a K''_a}{K_h K_t K_i} \tag{31}$$

From the two equations in eqn (31) K_i and K_{Ct/Ct^-} can be calculated. In conclusion, all equilibrium constants of kuromanin (or any other flavylium multistate of species exhibiting a high *cis–trans* isomerization rate) can be calculated by means of this procedure. In Table 1 all equilibrium constants of kuromanin are presented.

Moreover, from the data of Table 1 the mole fraction distribution of all species can be represented as in Fig. 3.

The knowledge of the equilibrium constants and the mole fraction distribution of anthocyanins is crucial information to rationalize the properties of these natural dyes mentioned in the introduction. Moreover, it is indispensable to understand the strategies used by nature to fix the colours. It will be the starting point of this perspective article to rationalize the strategies used by nature to fix the beautiful colours that paint the world.

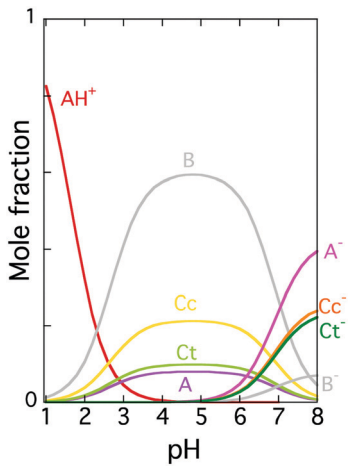

Fig. 3 Mole fraction distribution of kuromanin at the equilibrium.

5. Overcoming the physical–chemical limitations of anthocyanins to confer colour

5.1. Anthocyanins by themselves are unable to give significant colour in plants

The pH of the vacuoles where anthocyanins are located could change considerably. It could be as low as 2.0 in citrus fruits[17] or 7.7 in some flowers,[18] but a pH of approximately 5 is often observed.[19] In Fig. 4 the limitations of two representative anthocyanins are shown.

Inspection of Fig. 4 clearly shows that the domain of the red colour of the flavylium cation is limited to very low pH values, while the quinoidal base is a minor species at moderately acidic pH values. It is worthy of note that the anionic quinoidal base tends to be dominant for neutral or slightly basic pH values. However, in this case the anthocyanins are not stable and undergo degradation.[20]

5.2. Copigmentation: a simple way to increase the colour

Co-pigmentation is a term that accounts for the increasing colour caused by colourless compounds, such as amino acids, sugars and flavonoids.[21] Goto proposed a unified mechanism for co-pigmentation and self-association, which he called molecular stacking theory.[22–25] Therefore, the thermodynamic driving forces for co-pigmentation and self-association were considered by Goto to be the same: the hydrophobic aromatic residues assemble in aqueous solutions.[25] This theory was also extended to polyacylated anthocyanins.[23–25] It is known that copigmentation has a high impact on food colour, and its stability and intensity.[26] For instance, at wine pH (3.2–3.8), anthocyanins are predominantly present in their colourless neutral forms; however, the intense red colour displayed by young red wines is mainly due to the interaction of the flavylium cation of anthocyanins with other wine components including phenolic acids, flavanols and flavanones.[27–29]

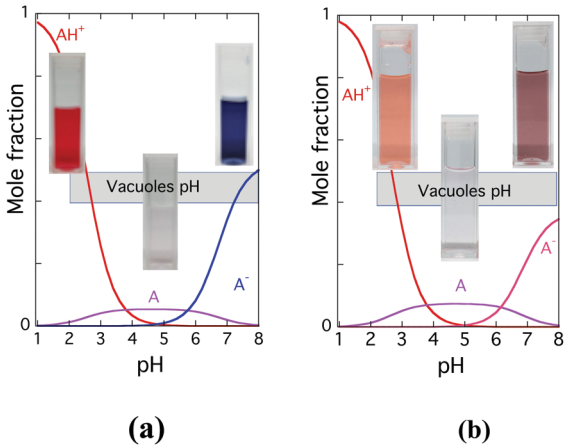

Fig. 4 (a) Mole fractions of the coloured forms of oenin and (b) the same for cyanidin. In this case the blue colour is observed only for the dianionic quinoidal base (not shown).

The limitations of the copigmentation models and the respective mathematical expressions were recently reported.[30] Initially copigmentation studies were limited to copigmentation with the flavylium cation and later with the quinoidal bases.[30,31] However, *a priori* there is no reason to exclude the existence of copigmentation with all species of the flavylium based multistate of species shown in Scheme 2. Eqn (32)–(34) describe these possible interactions.

For flavylium cation complexation

$$AH^+ + CP \rightleftharpoons AH^+CP \quad K_{AH+CP} \tag{32}$$

for the neutral species

$$X + CP \rightleftharpoons XCP \quad K_{XCP} \tag{33}$$

and for the anionic species

$$X^- + CP \rightleftharpoons X^-CP \quad K_{X^-CP} \tag{34}$$

with

$$X = AH^+, A, B, Cc \text{ and } Ct \tag{35}$$

This complex system can be once more simplified to a diprotic acid with eqn (32), (36) and (37)

$$CB + CP \rightleftharpoons CBCP \quad K_{CBCP} \tag{36}$$

$$CB^- + CP \rightleftharpoons CB^-CP \quad K_{CB^-CP} \tag{37}$$

From the definition of eqn (36) and using the set of eqn (33),[15] the equilibrium constant K_{CBCP} is defined by eqn (38).

$$K_{CBCP} = \frac{[CBCP]}{[CB][CP]} = \frac{K_{ACP}K_a + K_{BCP}K_h + K_{CcCP}K_hK_t + K_{CtCP}K_hK_tK_i}{K_a'} \tag{38}$$

Proceeding similarly to eqn (37) and the set of eqn (34), the equilibrium constant K_{CB^-CP} is defined by eqn (39).

$$K_{CB^-CP} = \frac{[CB^-CP]}{[CB^-][CP]} = \frac{K_{A^-CP}K_{A/A^-}K_a + K_{B^-CP}K_{B/B^-}K_h + K_{Cc^-CP}K_{Cc/Cc^-}K_hK_t + K_{Ct^-CP}K_{Ct/Ct^-}K_hK_tK_i}{K_a'K_a''} \tag{39}$$

As shown previously[15] the system behaves again as a diprotic acid with acidity constants given by eqn (40) and (41). See Appendix 2 for more details.

$$K'_{a(CP)} = \frac{K_a'(1 + K_{CBCP}[CP])}{1 + K_{AH^+CP}[CP]} \tag{40}$$

$$K''_{a(CP)} = \frac{K_a''(1 + K_{CB^-CP}[CP])}{1 + K_{CBCP}[CP]} \tag{41}$$

The mathematical model is valid for 1 : 1 copigmentation and excess copigment concentration ([CP]) in comparison with anthocyanin.

When reverse pH jumps are applied to study copigmentation, the pseudo equilibrium should be considered, the terms regarding Ct removed, and K_a', eqn (40), and K_a'', eqn (41), substituted by $K\hat{}_a$, eqn (42), and $K\hat{}\hat{}_a$, eqn (43), respectively.

$$K\hat{}_{a(CP)} = \frac{K\hat{}_a(1 + K_{CB\hat{}CP}[CP])}{1 + K_{AH^+CP}[CP]} \tag{42}$$

$$K\hat{}\hat{}_{a(CP)} = \frac{K\hat{}\hat{}_a(1 + K_{CB^-\hat{}CP}[CP])}{1 + K_{CB\hat{}CP}[CP]} \tag{43}$$

As shown above, the terms regarding AH^+ and A should be written together.

$$\chi_{AH^+} + \chi_{AH^+CP} + \chi_A + \chi_{ACP} + \chi_{A^-} + \chi_{ACP^-} = \frac{[H^+]^2 + a_{0(CP)}K\hat{}_{a(CP)}[H^+] + a_{1(CP)}K\hat{}_{a(CP)}K\hat{}\hat{}_{a(CP)}}{D\hat{}_{CP}} \tag{44}$$

$$D\hat{}_{CP} = [H^+]^2 + K\hat{}_{a(CP)}[H^+] + K\hat{}_{a(CP)}K\hat{}\hat{}_{a(CP)}$$

$$\chi_B + \chi_{BCP} + \chi_{B^-} + \chi_{BCP^-} = \frac{[H^+]^2 + b_{0(CP)}K\hat{}_{a(CP)}[H^+] + b_{1(CP)}K\hat{}_{a(CP)}K\hat{}\hat{}_{a(CP)}}{D\hat{}_{CP}} \tag{45}$$

$$\chi_{Cc} + \chi_{CcCP} + \chi_{Cc^-} + \chi_{CcCP^-} = \frac{[H^+]^2 + c_{0(CP)}K\hat{}_{a(CP)}[H^+] + c_{1(CP)}K\hat{}_{a(CP)}K\hat{}\hat{}_{a(CP)}}{D\hat{}_{CP}} \tag{46}$$

The copigmentation constants with all species of the multistate are based on the determination of the coefficients $a_{n(CP)}$, $b_{n(CP)}$, $c_{n(CP)}$ with n = 0, 1. Comparing the mole fractions written in terms of the coefficients $a_{n(CP)}$, $b_{n(CP)}$, $c_{n(CP)}$ and those based on the equilibrium constants allows for the definition of the equalities shown in eqn (47).[15] See Appendix 2 for more details.

The expressions presented in eqn (47) allow for the determination of all copigmentation constants provided that the

$$\begin{aligned}
a_{0(CP)}K\hat{}_1 &= \frac{K_a + K_{ACP}K_a[CP]}{1 + K_{AH^+CP}[CP]};\\
a_{1(CP)}K\hat{}_1K\hat{}_2 &= \frac{K_{A/A^-}K_a + A_{ACP/ACP^-}K_{ACP}K_a[CP]}{1 + K_{AH^+CP}[CP]};\\
b_{0(CP)}K\hat{}_1 &= \frac{K_h + K_{BCP}K_h[CP]}{1 + K_{AH^+CP}[CP]};\\
b_{1(CP)}K\hat{}_1K\hat{}_2 &= \frac{K_{B/B^-}K_h + K_{BCP/BCP^-}K_{BCP}K_h[CP]}{1 + K_{AH^+CP}[CP]};\\
c_{0(CP)}K\hat{}_1 &= \frac{K_hK_t + K_{CcCP}K_hK_t[CP]}{1 + K_{AH^+CP}[CP]};\\
c_{1(CP)}K\hat{}_1K\hat{}_2 &= \frac{K_{Cc/Cc^-}K_hK_t + K_{CcCP/CcCP^-}K_{CcCP}K_hK_t[CP]}{1 + K_{AH^+CP}[CP]}
\end{aligned} \tag{47}$$

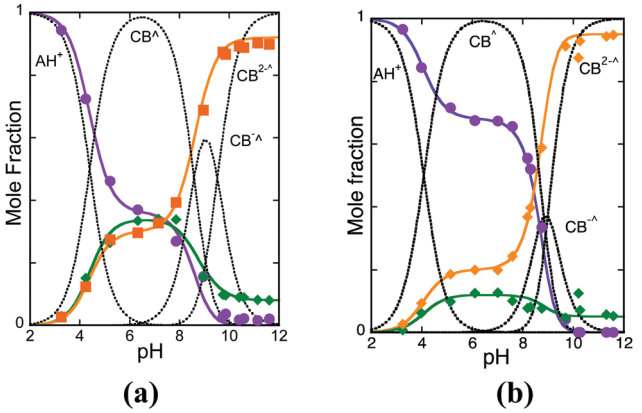

Fig. 5 (a) Mole fraction distribution of 4′-hydroxyflavylium and (b) the same in the presence of caffeine 0.058 M. (●) $AH^+ + A + A^-$; (◆) $B + B^-$; (■/◆) $Cc + Cc^-$.

constants K_a, K_h and K_t were determined in the absence of the copigment, and K_{AH^+CP} is calculated from UV-vis measurements at pH = 1, eqn (48)

$$A_\lambda = \frac{A_0 + A_f K_{AH^+CP}[CP]}{1 + K_{AH^+CP}[CP]} \quad (48)$$

where A_0 is the absorbance in the absence of the copigment, and A_f the absorbance of the plateau. If the plateau is not achieved the fitting of A_f and K_{AH^+CP} should be made.

The mole fractions of the *trans*-chalcones are obtained from the reverse pH jumps in the presence of the copigment monitored by a standard spectrophotometer.

$$d_{0(CP)}K'_{a(CP)} = \frac{K_h K_t K_i + K_{CtCP} K_h K_t K_i[CP]}{1 + K_{AH^+CP}[CP]} \quad (49)$$

$$d_{1(CP)}K'_{a(CP)}K''_{a(CP)} = \frac{K_{Ct/Ct^-} K_h K_t + K_{CtCP/CtCP^-} K_{CtCP} K_h K_t K_i[CP]}{1 + K_{AH^+CP}[CP]} \quad (50)$$

The model was tested with the compound 4′-hydroxyflavylium and oenin with caffeine.[15]

Differently from the simpler anthocyanins such as oenin or kuromanin, 4′-hydroxyflavylium is stable in basic medium. The equilibrium is difficult to attain (needs high temperature) and occurs between the flavylium cation and *trans*-chalcones. However, the pseudo equilibrium is constituted of similar mole fractions of B, Cc and Ct, Fig. 5a, a convenient situation to account for the copigmentation constants with these forms. The results are shown in Fig. 5, Tables 2 and 3.

Table 3 Co-pigmentation constants (M^{-1}) of the model compound 4′-hydroxyflavylium with caffeine

K_{AH^+CP}	K_{ACP}	K_{BCP}	K_{B^-CP}	K_{CcCP}	K_{Cc^-CP}	K_{CtCP}[a]	K_{Ct^-CP}[a]
18	134	13	9	42	44	47	94

[a] Measured at the equilibrium; the estimated error for neutral species is 10% but for anionic it is higher (not estimated)

Due to the existence of a single hydroxy substitution the anionic quinoidal base of this compound is not available. Another characteristic is that anionic hemiketal is a minor species, with anionic *cis*-chalcone the dominant, Fig. 5a. The copigmentation with the neutral quinoidal base and caffeine is very efficient and very significant with the chalcones.

The model was also applied to the complexation of oenin with caffeine, Fig. 6.

The oenin copigmentation with caffeine is illustrative of the potential of copigmentation to confer colour to anthocyanins as well as to identify the respective limitations. Calculation of the mole fraction of the *trans*-chalcones was carried out by a reverse pH jump followed by a standard spectrophotometer. The time to reach the equilibrium is relatively long in the case of oenin especially at higher pH values. Moreover, is precisely at these pH values that common anthocyanins are more unstable. Consequently, there is higher uncertainty at higher pH values as indicated by the yellow band in the graphics. Nevertheless, the difference between pseudo equilibrium and equilibrium is small.

Copigmentation is able to increase the pH domain of the flavylim cation and also increase the mole fraction distribution of the quinoidal base. There is a tendency for the anionic quinoidal base to be the dominant species at higher pH values, but copigmentation does not seem to be very efficient to prevent degradation, while there is a lack of studies relating copigmentation with anthocyanin stabilization.

5.3. Acylated anthocyanins

The sugars of anthocyanins can be acylated with cinnamic acids (*e.g.*, caffeic, coumaric, ferulic, and sinapic acids) or aliphatic acids (*e.g.*, acetic, malic, oxalic, and succinic acids).[11] This opens the possibility of intramolecular copigmentation involving these acylated residues and the core of the flavylium cation.

Table 2 Equilibrium constants of 4′-hydroxyflavylium. K_h is given in M units. Estimated error 10%

pK'_a	pK''_a	pK'''_a	$pK^{\wedge}{}_a$	$pK^{\wedge\wedge}{}_a$	$pK^{\wedge\wedge\wedge}{}_a$	pK_a	K_h (M)	K_t	K_i
3.3[a]	8.1	9.25	4.4	8.6	9.5	4.8	1.4×10^{-5}	0.88	37[a]

pK_{B/B^-}	$pK_{B^-/B2^-}$	pK_{Cc/Cc^-}	$pK_{Cc^-/Cc2^-}$	pK_{Ct/Ct^-}	$pK_{Ct^-/Ct2^-}$
8.95	9.8	8.1	9.5	8.1	9.5

[a] Approximate values.

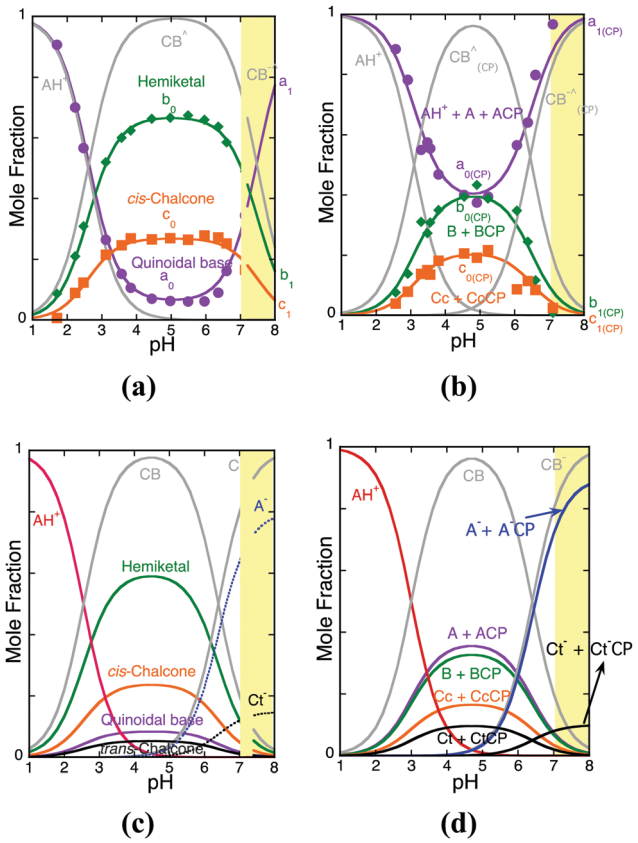

Fig. 6 (a) Mole fraction distribution of oenin at the pseudo-equilibrium; (b) the same in the presence of caffeine 0.058 M; (c) the same as (a) at the equilibrium; and (d) the same as (b) at the equilibrium. In (a) and (b) the representation refers to the three amplitudes observed in the reverse pH jumps monitored by stopped flow. The mole fractions inside the yellow band have more uncertainty, in particular at the equilibrium.

A beautiful example of this type of compound was studied by Kondo *et al.*,[32] Scheme 3, who reported the structure of anthocyanin extracted from the flowers of morning glory (*Ipomoea tricolor*). They observed that it is the same anthocyanin that gives the purple colour to the buds and the blue colour to the flowers and early associated the extended pH domain of the colour with the π-stacking interaction of the acylated residues with the flavylium core, Scheme 4.[18,23]

The power of physical chemistry in the comprehension of these systems is stressed when the mole fraction distribution of pigment 3 of Scheme 3 is presented (Fig. 7). The mole fraction distribution of the species was calculated as described above. In this case it is indispensable to extend the study at higher pH values, which is possible in this compound at least for the pseudo-equilibrium, because the intermolecular copigmentation not only increases the mole fraction distribution of the quinoidal base and its anionic form, but also increases their stability.[33]

Considering that hydration of the quinoidal base does not take place in acidic medium, a breakthrough discovered by Brouillard and Dubois,[34] the disappearance of the coloured species, the flavylium cation and quinoidal base, takes place from the hydration of the flavylium cation, eqn (2). The effect of the intramolecular copigmentation is also observed in the kinetic process. The rate constants k_h and k_{-h}, see eqn (2), increase and decrease, respectively, from pigment 1 to pigment 2 to pigment 3, *i.e.* with the number of acylated units.

In Scheme 4 the sketch illustrates the effect of the triacylated sugar that surrounds the flavylium core protecting it from hydration.

The representation of the mole fraction distribution reported in Fig. 7 also explains how the same anthocyanins could give the purple colour to buds and blue to flowers. At approximately pH = 7, relatively small changes in pH could lead to large colour changes from purple to blue. Vacuolar pH measurements of morning glory petals in the abaxial epidermis have shown that the purplish red buds, purple flowers and blue open flowers were at pH = 6.6, 6.9, and 7.7, respectively.[18] Moreover, the spectra of pigment 3 in aqueous solutions at pH values of 7.68 and 6.37 corresponded to the reflective spectra of the open petal and bud, respectively.[18]

The effect of the number of acylated units is explained in the energy level diagram of Scheme 5.

In Scheme 5 the energy level diagram of pigment 3 was compared with previous work by Dangles *et al.*,[36] where the hydration constants $K_h(1 + K_t)$ were reported for the anthocyanins

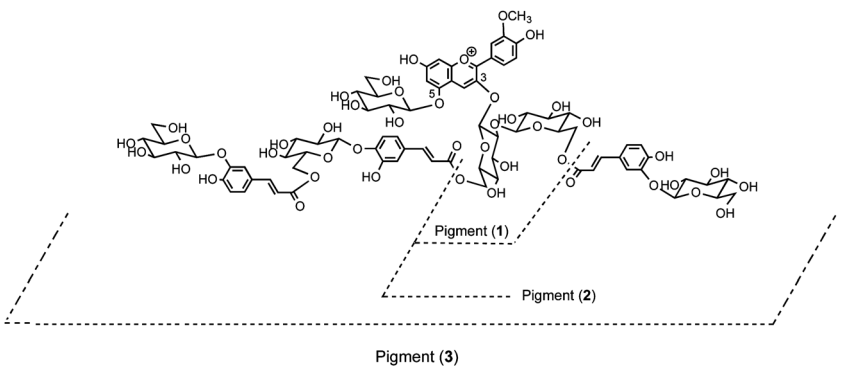

Scheme 3 Acylated anthocyanin extract from the flowers of morning glory (*Ipomoea tricolor*) and related derivatives. The same anthocyanin, pigment 3, gives the purple colour to the buds and the blue colour to the flowers.

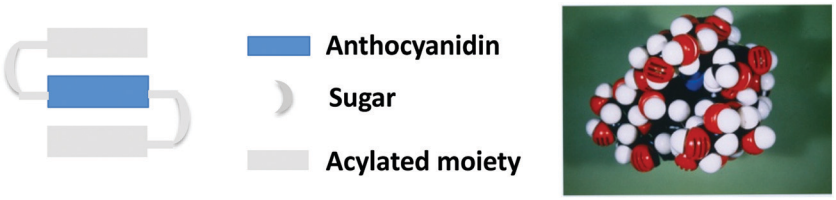

Scheme 4 Sketch representing the intramolecular copigmentation in polyacylated anthocyanins; CPK models of heavenly blue anthocyanin adapted from ref. 23 and 32. Copyright © 2019 American Chemical Society.

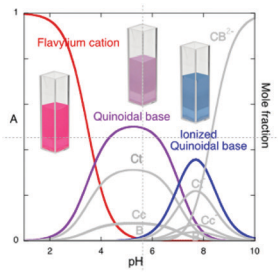

(a)

Rate constants of hydration		
	k_h/s^{-1}	$k_{-h}/M^{-1}\,s^{-1}$
Pigment 1	0.35	43
Pigment 2	0.12	145
Pigment 3	0.01	377

(b)

Fig. 7 (a) Mole fraction distribution of the blue anthocyanin (*Ipomoea tricolor*) including the anionic forms and (b) rate constants of hydration (k_h) and dehydration (k_{-h}).

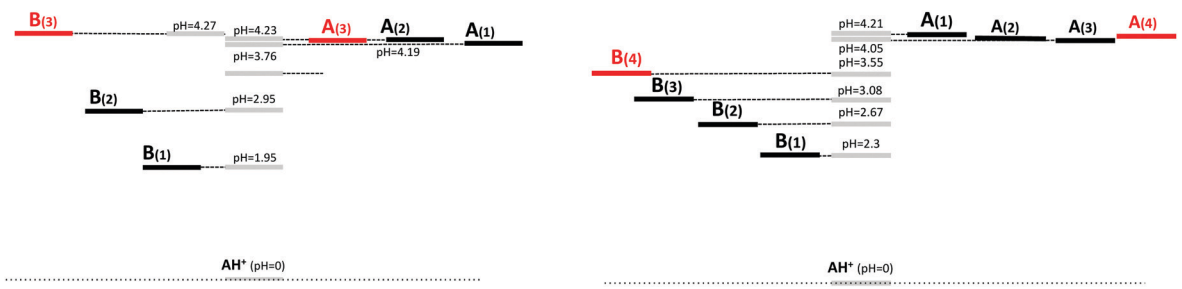

Scheme 5 (a) Quinoidal base and hemiketal energy level diagram constructed with the equilibrium constants reported by Mendoza *et al.*[35] and (b) the same as (a) using the data reported by Dangles *et al.*[36] In both energy level diagrams, B actually corresponds to B + Cc. This notation was required to accurately compare both diagrams due to the fact that the apparent hydration constants reported by Dangles *et al.*[36] correspond to $K_h(1 + K_t)$.

extracted from another morning glory variety, the flower of *Pharbitis Ipomoea nil* (a pelargonidin derivative), Scheme 6.

Inspection of Scheme 5 clearly shows that the energy level diagram of the quinoidal base is only slightly affected by the acylated units. However, there is a dramatic destabilization of hemiketal with the number of acylated units. It is worthy of note that only for three acylated units the quinoidal base becomes more stable than hemiketal. The destabilization of hemiketal is also observed by the values of the hydration rate constants shown in Fig. 7. An increasing number of acylated units decreases the hydration and increases the dehydration constants.

5.4. Metal interaction

Polyphenols bearing a catechol unit are known to efficiently coordinate metals and have been used as sequestering agents for very toxic metals such as Be^{2+}[37] and Zr^{4+}[38] or to complex Al^{3+} in the case of quercetin,[39] isoquercitrin,[40] luteolin,[41] and caffeic acid.[42] In particular, studies of aluminium complexes with catechol and hydroxyflavones were reported.[43,44] Anthocyanins and related compounds possessing a catechol unit are also able to complex metal oxides, for example titanium dioxide in Dye Sensitized Solar Cells (DSSCs) functioning in this way as light absorbers.[45]

In anthocyanins and related compounds metal complexation is achieved very efficiently through the chelate catechol unit in ring B, as in cyanidin, delphinidin and petunidin. In synthetic flavylium compounds the catechol unit can also be inserted in ring A. It is the case of 4-methyl-7,8-dihydroxyflavylium, Scheme 7.

5.4.1. Complexation with aluminium. In principle the catechol unit can form 1:1, 1:2 and 1:3 (metal:ligand)

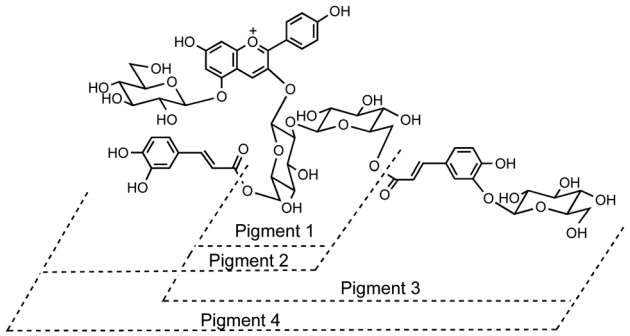

Scheme 6 Acylated anthocyanin extracted from another morning glory variety, the flower of *Pharbitis Ipomoea nil* (a pelargonidin derivative) and respective derivatives.

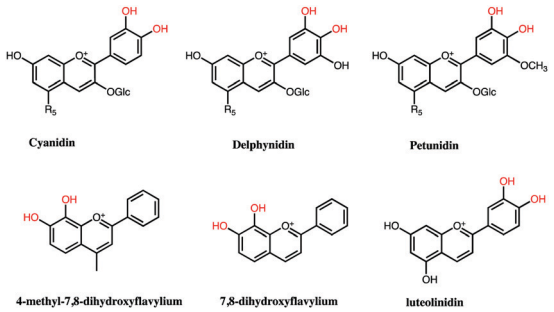

Scheme 7 Natural and synthetic flavylium compounds possessing a very appropriate chelate unit (two adjacent hydroxy substituents) to bind metals (R_5 = H, monoglucosides; R_5 = OGlc diglucosides).

complexes as observed in the case of $Al^{3+}$and caffeic acid.[42] Using a large excess of aluminium the formation of the 1 : 1 complex is favourable.

In the case of aluminum cations in water, the primary hydration shell consists of six water molecules in octahedral coordination. These water molecules are polarized due to the high charge of the metal and a pH increase can give rise to the loss of protons, eqn (51)–(54).[46]

$$Al(H_2O)_6^{3+} + H_2O \rightleftharpoons Al(H_2O)_5(OH)^{2+} + H_3O^+ \quad pK_{a1} = 4.95 \tag{51}$$

$$Al(H_2O)_5(OH)^{2+} + H_2O \rightleftharpoons Al(H_2O)_4(OH)_2^{+} + H_3O^+ \quad pK_{a2} = 5.6 \tag{52}$$

$$Al(H_2O)_4(OH)_2^{+} + H_2O \rightleftharpoons Al(H_2O)_3(OH)_3 + H_3O^+ \quad pK_{a3} = 6.7 \tag{53}$$

$$Al(H_2O)_3(OH)_3 + H_2O \rightleftharpoons Al(H_2O)_2(OH)_4^{-} + H_3O^+ \quad pK_{a4} = 5.6 \tag{54}$$

The mole fraction distribution of aluminum species in water is shown in Fig. 8.[46]

5.4.1.1. Catechol complexation with aluminium[43]. Previous work using potentiometric and conductometric methods indicates that the complexation of catechol with aluminium takes place between the fully deprotonated form of the ligand and Al^{3+}.[43]

$$K = \frac{[Al(Catechol)^+][H^+]^2}{[Al^{3+}][H_2(Catechol)]}; \quad K_1 = \frac{K}{K_{a1}K_{a2}} \tag{55}$$

$$H_2Catechol + H_2O \overset{K_{a1}}{\rightleftharpoons} HCatechol^- + H_3O^+ \quad pK_{a1} = 9.44^{43} \tag{56}$$

$$HCatechol^- + H_2O \overset{K_{a2}}{\rightleftharpoons} Catechol^{2-} + H_3O^+ \quad pK_{a2} = 12.8^{43} \tag{57}$$

$$Al^{3+} + Catechol^{2-} \overset{K_1}{\rightleftharpoons} Al(Catechol)^{2-} \quad \log K_1 = 16.24^{43} \tag{58}$$

In conclusion the interaction of the fully deprotonated form of catechol exhibits an extremely strong association constant and the equilibrium is established between the fully protonated form of catechol (H_2Catechol) and the complex ($Al(Catechol)^{2-}$) and consequently the concentrations of the species $HCatechol^-$ and $Catechol^{2-}$ are neglected.

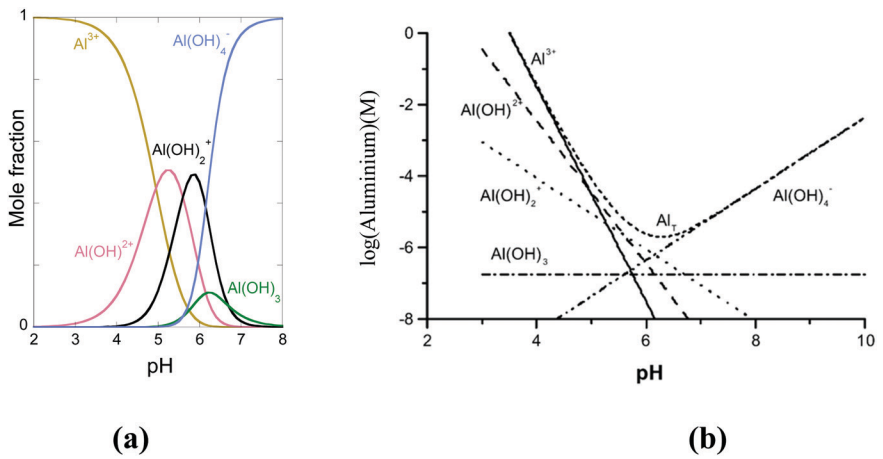

Fig. 8 (a) Mole fraction distribution of Al(III) in water and (b) concentrations of monomeric hydrolysis products of Al(III) in equilibrium with the amorphous hydroxides, at zero ionic strength and 25 °C. Adapted from ref. 46.

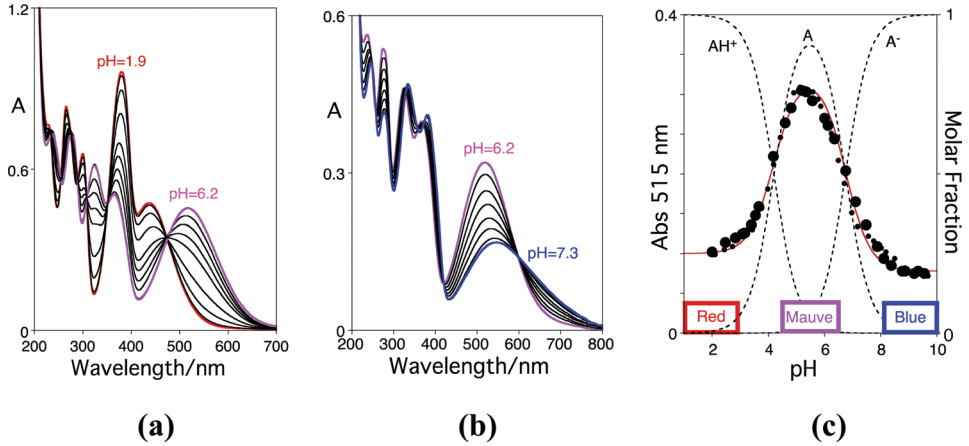

Fig. 9 (a) Spectral variations corresponding to the acid–base equilibrium between AH^+ and A (pK_a = 4.0); (b) the same for the equilibrium between A and A^- (pK_{A/A^-} = 6.8); and (c) the mole fraction distribution of the species of 4-methyl, 7,8-dihydroxyflavylium.

5.4.1.2. 4-Methyl-7,8-dihydroxyflavylium. 4-Methyl-7,8-dihydroxyflavylium, as other flavylium cations possessing an alkyl substituent in position 4, does not hydrate in water and only the flavylium cation and quinoidal base are present in all the pH range. 4-Alkylflavylium compounds are excellent models to study the effect of metal complexation in achieving colour particularly with anionic quinoidal bases.[47]

In Fig. 9 the spectral modification of the compound 4-methyl-7,8-dihydroxyflavylium is shown. The existence of two acid base equilibria with acidity constants pK_a = 4.0 and pK_{A/A^-} = 6.8 is clear.

5.4.1.3. Complexation of aluminium with 4-methyl-7,8-dihydroxyflavylium[48,49]. The spectral variations as a function of pH are shown in Fig. 10. The existence of isosbestic points indicates an equilibrium between the flavylium cation and an aluminium complex.

Theory. The system can be accounted for by means of eqn (59)–(61).

$$AH^+ + H_2O \rightleftharpoons A + H_3O^+ \quad K_a \text{ proton transfer} \quad (59)$$

$$A + H_2O \rightleftharpoons A^- + H_3O^+ \quad K_{A/A^-} \text{ proton transfer} \quad (60)$$

$$A^- + Al^{3+} \rightleftharpoons Al^{3+}A^- \quad K_{CP(A^-)} = \frac{[Al^{3+}A^-]}{[Al^{3+}][A^-]} \text{ complexation} \quad (61)$$

As shown in Appendix 3 the concentration of the flavylium cation is given by a quadratic equation, eqn (62)

$$\gamma\beta[AH^+]^2 + (\alpha\beta + \gamma C_{0(Al)} - \gamma C_{0(antho)})[AH^+] - \alpha C_{0(antho)} = 0 \quad (62)$$

with α, β, and γ defined by eqn (63)–(65), respectively

$$\alpha = 1 + \frac{K_{a1}}{[H^+]} + \frac{K_{a1}K_{a2}}{[H^+]^2} + \frac{K_{a1}K_{a2}K_{a3}}{[H^+]^3} + \frac{K_{a1}K_{a2}K_{a3}K_{a4}}{[H^+]^4} \quad (63)$$

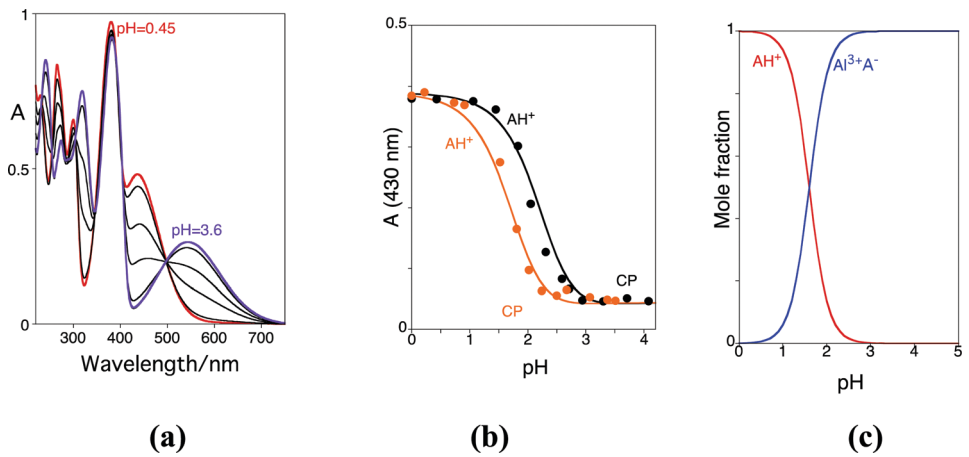

Fig. 10 (a) Spectral variations of the compound 4-methyl, 7,8-dihydroxyflavylium 5×10^{-5} M in the presence of aluminum chloride 5×10^{-2} M for the following pH values: 0.45; 1.2; 1.66; 2.4; 2.88; and 3.6. (b) pH dependence of the absorbance at 430 nm of the compound 4-methyl, 7,8-dihydroxyflavylium. Fitting was achieved by means of eqn (67) for c_1 = 0.398, c_4 = 0.05, Al^{3+} = 0.2 M (orange) and aluminum chloride 0.02 M (black). (c) Mole fraction distribution of the flavylium cation and the $Al^{3+}A^-$ complex, for aluminum chloride 0.2 M.

$$\beta = 1 + \frac{K_a}{[H^+]} + \frac{K_{A/A^-}K_a}{[H^+]^2} \quad (64)$$

$$\gamma = K_{CP(A^-)}\frac{K_{A/A^-}K_a}{[H^+]^2} \quad (65)$$

$C_{0(Al)}$ and $C_{0(antho)}$ are respectively the total concentrations of the metal and anthocyanin.

All parameters in eqn (58) except $K_{CP(A^-)}$ are known (calculated in the absence of the metal) and a fitting of the experimental data only needs to adjust this constant, which allows for the determination of the mole fraction distribution of the complex. Moreover, once the mole fraction of the free flavylium cation is calculated (by fitting, see below) the mole fractions of all the other species A, B, Cc and Ct through eqn (1)–(4) and A^-, B^-, Cc^- and Ct^- by means of eqn (9)–(12) are obtained. A final verification can be done because the sum of all the mole fractions involving anthocyanins should be equal to unity.

The variation of the absorbance at longer wavelengths *versus* pH is accounted for by means of eqn (66)

$$A_\lambda = \varepsilon_{AH^+}[AH^+] + \varepsilon_A[A] + \varepsilon_{A^-}[A^-] + \varepsilon_{Al^{3+}A^-}[Al^{3+}A^-] \quad (66)$$

which can be written as in eqn (67)

$$\begin{aligned} A_\lambda &= c_1\chi_{AH^+} + c_2\chi_A + c_3\chi_{A^-} + c_4\chi_{Al^{3+}A^-} \\ c_1 &= \varepsilon_{AH^+}C_{0(Antho)}; \quad c_2 = \varepsilon_A C_{0(Antho)}; \\ c_3 &= \varepsilon_{A^-}C_{0(Antho)}; \quad c_4 = \varepsilon_{AH^+A^-}C_{0(Antho)} \end{aligned} \quad (67)$$

where ε stands for the mole absorption coefficient of the flavylium cation, quinoidal base, anionic quinoidal base and the 1 : 1 complex $Al^{3+}A^-$, the species that absorb light at longer wavelengths, and χ is the respective mole fraction. (In the case of very high complexation constants the mole fractions of A and A^- can be neglected.) For more details see Appendix 3.

Table 4 4-Methyl-7,8-dihydroxyflavylium in the absence and presence of the metal

pK_a	pK_{A/A^-}	$\log K_{CP(A^-)}$
4.0	6.8	8.3

The fitting of the data reported in Fig. 10 was achieved by means of eqn (67) using the quadratic eqn (62), to calculate the free flavylium cation and metal, and consequently all the species absorbing in the visible, for the parameters $c_1 = 0.398$, $c_2 = c_3 = 0$, $c_4 = 0.05$, at 430 nm, and $K_{CP} = 2 \times 10^8\ M^{-1}$ and for a total concentration of the compound of 5×10^{-5} M, independently of the metal concentration in excess.

Simplification of the system. It is straightforward to prove that when the complexation constant is very high the mole fraction of the free A and A^- can be neglected (as in the case of catechol described above) and eqn (68) can be used.

$$A_\lambda = c_1\chi_{AH^+} + c_4\chi_{A^-Al(III)} \quad (68)$$

The fitting reported in Fig. 10 was achieved for $pK_a = 4$, $pK_{A/A^-} = 6.8$ and $K_{CP} = 2 \times 10^8\ M^{-1}$, Table 4, and $c_1 = 0.385$ and $c_4 = 0.05$, the same parameters reported above. This approximation was previously reported.[47]

5.4.1.4. 7,8-Dihydroxyflavylium in the absence of the metal. The absorption spectra of the compound 7,8-dihydroxyflavylium taken 10 ms after direct pH jumps from pH = 1.0 monitored by stopped flow are shown in Fig. 11.

Presentation of the absorbance at 542 nm *versus* pH allows for the determination of $pK_a = 3.8$ and $pK_{A/A^-} = 9.7$. In Fig. 12 the spectral variations at the equilibrium are shown. The quinoidal base almost disappears. It is a small shoulder of the spectrum at pH = 4.4. The equilibrium species at this pH value is the *trans*-chalcone as observed for other flavylium compounds bearing a hydroxyl substituent in position 7. For pH > 4.4 the isosbestic points are not formed indicating as expected that more than one species is formed. The titration curves reported in Fig. 12c show that three acid base constants are observed $pK_a' = 2.4$; $pK_a'' = 6.6$; and $pK_a''' = 9.4$. The situation can be summarized in eqn (69) and (70).

$$AH^+ \rightleftharpoons A \rightleftharpoons A^- \quad 10\ ms\ after\ direct\ pH\ jump \quad (69)$$

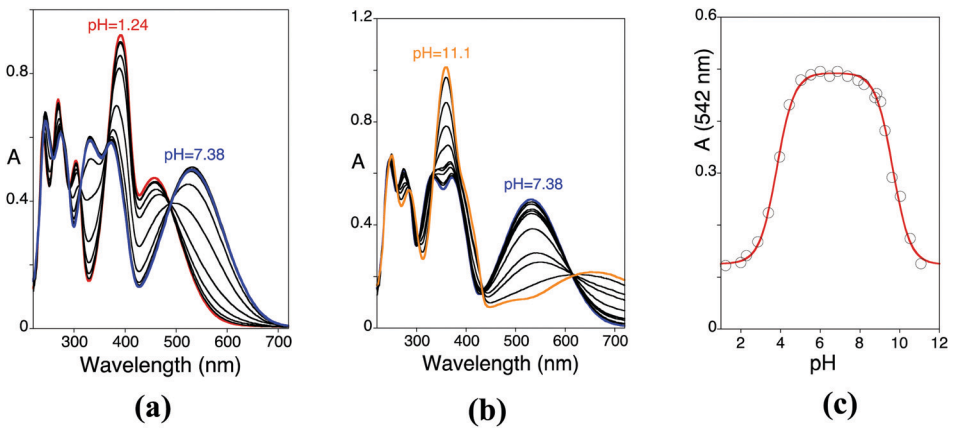

Fig. 11 Spectral variations of the compound 7,8-dihydroxyflavylium taken 10 ms after direct pH jumps from equilibrated solutions at pH = 1 to (a) 1.24 < pH < 7.38 and (b) 7.38 < pH < 11.1 and (c) the titration curve at 542 nm allowing for the determination of $pK_a = 3.8$ and $pK_{A/A^-} = 9.7$.

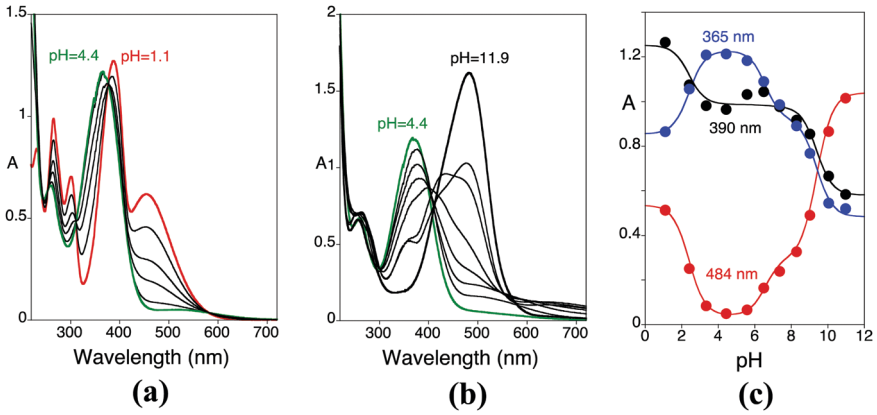

Fig. 12 Spectral variations of the compound 7,8-dihydroxyflavylium at the equilibrium (a) 11.1 < pH < 4.4 and (b) 4.4 < pH < 11.99 and (c) variation of the absorbance of 7,8-dihydroxyflavylium at the equilibrium; $pK_a^{'} = 2.05$; $pK_a^{''} = 6.6$; $pK_a^{'''} = 9.4$.

$$\underset{\text{equilibrium}}{AH^+} \overset{K_a^{'}}{\rightleftharpoons} A(\text{minor}) + Ct \overset{K_a^{''}}{\rightleftharpoons} Ct^- \overset{K_a^{'''}}{\rightleftharpoons} Ct^{2-} \qquad (70)$$

The ratio $K_a/K_a^{'} = 0.022$ gives the mole fraction of A in CB and the other component is Ct.

Moreover, the ratio $\chi_{Ct} = \dfrac{K_h K_t K_i}{K_a^{'}} = 0.978$ in Fig. 12 leads to the product of the constants $K_h K_t K_i = 8.7 \times 10^{-3}$.

On the other hand, $K_a^{''}$, eqn (71), and $K_a^{'''}$, eqn (73), can be simplified to eqn (72) and (74)

$$K_a^{''} = \frac{K_{A/A^-} K_a + K_{B/B^-} K_h + K_{Cc/Cc^-} K_h K_t + K_{Ct/Ct^-} K_h K_t K_i}{K_a^{'}} \qquad (71)$$

$$K_a^{''} = \frac{K_{A/A^-} K_a + K_{Ct/Ct^-} K_h K_t K_i}{K_a^{'}} \qquad (72)$$

allowing for calculation of $K_{Ct/Ct^-} K_h K_t K_i = 2.23 \times 10^{-9}$ $M^2$and $pK_{Ct/Ct^-} = 6.6$

$$K_a^{'''} = \frac{K_{A^-/A^{2-}} K_{A/A^-} K_a + K_{B^-/B^{2-}} K_{B/B^-} K_h + K_{Cc^-/Cc^{2-}} K_{Cc/Cc^-} K_h K_t + K_{Ct^-/Ct^{2-}} K_{Ct/Ct^-} K_h K_t K_i}{K_a^{'} K_a^{''}} \qquad (73)$$

$$K_a^{'''} = \frac{K_{Ct^-/Ct^{2-}} K_{Ct/Ct^-} K_h K_t K_i}{K_a^{'} K_a^{''}} = 3.98 \times 10^{-10}\ M \qquad (74)$$

There is no A^{2-} in this compound for structural reasons and CB^{2-} is equal to Ct^{2-}.

Giving $K_{Ct^-/Ct^{2-}} K_{Ct/Ct^-} = 9.95 \times 10^{-16}$ M^2 determination of $pK_{Ct^-/Ct2^-} = 9.4$ is obtained.

This compound similarly to other 7-hydroxyflavylium derivatives exhibits an equilibrium between AH^+ and *trans*-chalcones (Table 5).

Table 5 7,8-Dihydroxyflavylium in the absence of the metal

pK_a	pK_{A/A^-}	$pK_a^{'}$	$pK_a^{''}$	$pK_a^{'''}$
3.8	9.7	2.4	6.6	9.4

5.4.1.5. 7,8-Dihydroxyflavylium in the presence of Al^{3+}. The question that is posed is if complexation takes place with A^- or if any other mono-anionic species, in particular Ct^-, also have significant complexation with the metal.

When a direct pH jump from a solution of 7,8-dihydroxyflavylium in the presence of Al^{3+} 0.1 M to pH = 2.8 is performed the initial solutions become pink in a few seconds and the absorption spectrum shown in Fig. 14a decreases slightly with a first order kinetic process with rate constant 1.3×10^{-3} s^{-1}. We interpret this process as the formation of a very small fraction of $Al^{3+}Ct^-$. This interpretation was corroborated by the two experiments reported in Fig. 14c and d. In Fig. 14c the spectral variations of 7,8-dihydroxyflavylium in the absence of the metal upon a direct pH jump to pH = 6 are shown. The initial spectra correspond to the quinoidal base that evolves to a mixture of *trans*-chalcone and anionic *trans*-chalcone (see Fig. 13). After addition of Al^{3+} (final concentration 0.1 M) to this equilibrated solution, the *trans*-chalcones give the same complex as Fig. 14a. The rate constants of the kinetics are the same within the experimental error and correspond to the kinetics of the *cis–trans* isomerization. In conclusion, the complexation of 7,8-dihydroxyflavylium occurs with the anionic form of the anthocyanin model compound, similarly to 4-methyl-7,8-dihydroxyflavylium and anthocyanins.

In Fig. 15 the spectral variations of 7, 8 dihydroxyflavylium in the presence of aluminium 0.1 M are shown. The spectral variations are similar to those presented by 4-methyl-7,8-dihydroxyflavylium in accordance with the formation of the 1 : 1 complex with the anionic quinoidal base.[50]

At higher pH values other spectral variations are observed indicating that complexation with other forms of 7,8-dihydroxyflavylium may occur. The situation becomes more complex because the hydroxyl species of the metal start to appear.

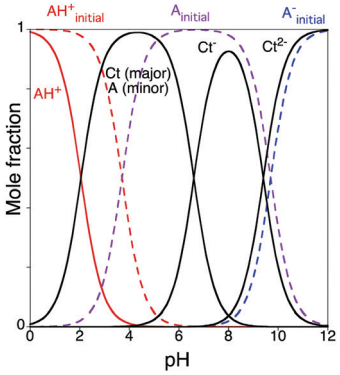

Fig. 13 Mole fraction distribution of the compound 7,8-dihydroxyflavylium after 10 ms (dotted lines) and at the equilibrium (solid lines).

We restricted our investigation of the complexation with this metal to pH < 4, to compare with the data reported for the complexation of this metal in *Hydrangea*,[50] see below.

Simplification of the system. In this case the mole fraction distributions of the flavylium cation in equilibrium with the $A^{-}Al^{3+}$ complex are given by eqn (75) and (76), respectively, and the absorbance *versus* pH by eqn (77), see the appendix.

$$\chi_{AH^+} = \frac{[H^+]^2}{[H^+]^2 + K_a'[H^+] + K_a'K_a'' + K_aK_{A/A^-}K_{CP(A^-)}[Al^{3+}]} \quad (75)$$

$$\chi_{A^-Al(III)} = \frac{K_aK_{A/A^-}K_{CP}[Al^{3+}]}{[H^+]^2 + K_a'[H^+] + K_a'K_a'' + K_aK_{A/A^-}K_{CP(A^-)}[Al^{3+}]} \quad (76)$$

$$A_\lambda = c_0\chi_{AH^+} + c_3\chi_{A^-Al(III)} \quad (77)$$

The colour of *Hydrangea Macrophylla* sepals (sterile "flowers", *i.e.* modified leaves) has been an intriguing question. It can assume a variety of red, purple and blue colours, depending on many variables, in particular the acidity of the soils.[49,50] Early it was discovered that Al^{3+} plays an essential role and that it is the same anthocyanin that confers colour, delphinidin-3-glucoside. The presence of the copigments neochlorogenic acid, 5-*O*-*p*-coumaroylquinic acid and chlorogenic acid was also observed. The blue sepals occur when the soil is acid and in basic soils only the red sepals are observed.[50] This was rationalized by the availability of Al^{3+}, which in basic soils is not soluble in water.

Schreiber *et al.* reported on the Al(III)–delphinidin complex in acidic ethanol (Scheme 8). According to these authors "A quinoidal base anion of delphinidin forms a primary complex with Al^3, and further a flavylium cation of delphinidin associates (by charge transfer and π–π interaction) with the quinoidal base anion".[49]

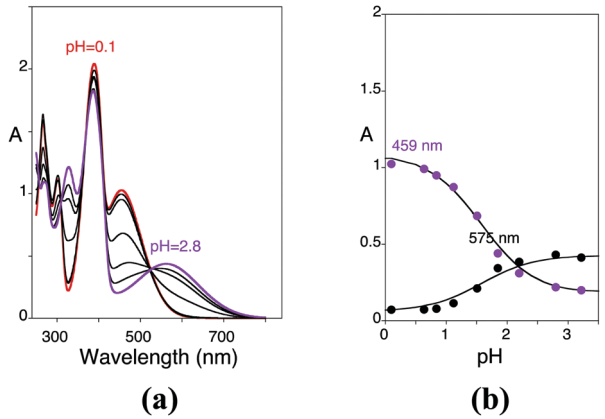

Fig. 15 (a) Spectral variations of 7,8-dihydroxyflavulium (1×10^{-4} M) in the presence of Al^{3+} 0.05 M. (b) Fitting of the absorbance at 459 nm and 575 nm *versus* pH, achieved according to eqn (25) for $a_1 = 1.02$ and $a_2 = 0.23$ for 459 nm and $a_1 = 0.08$ and $a_2 = 0.43$ for 575 nm. The same complexation constant $\log K_{CP(A^-)} = 10.3$ was achieved with the complete set of equations or through the simplified form, using the data of Table 2. The value for the constant $K_{CP(A^-)}$ corrects that previously reported in reference[47] ($\log K_{CP(A^-)} = 9.1$).

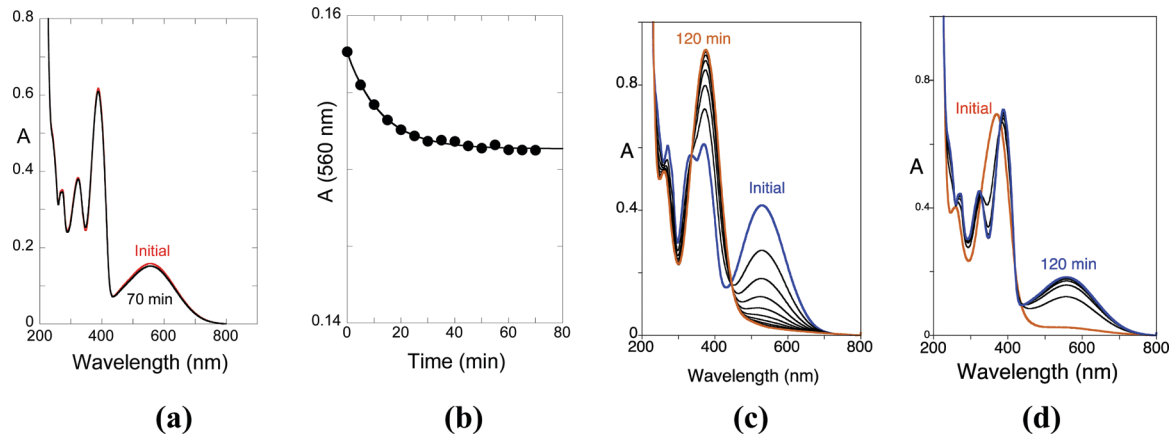

Fig. 14 (a) Spectral variations after a direct pH jump from a solution containing 7,8-dihydroxyflavylium and $[Al^{3+}] = 0.1$ M at pH = 1.0 to pH = 2.8. (b) Trace of the absorption at 560 nm showing that the initial complex is basically the one of the equilibrium and only 4% of the other complex is formed ($k_{obs} = 1.3 \times 10^{-3}$ s^{-1}). (c) Spectral variations of 7,8-dihydroxyflavylium (in the absence of the metal) upon a direct pH jump from pH = 1 to pH = 6 ($k_{obs} = 1.6 \times 10^{-3}$ s^{-1}). (d) Spectral variations after addition of Al^{3+} (final concentration 0.1 M, pH = 1.99, $k_{obs} = 1.5 \times 10^{-3}$ s^{-1}).

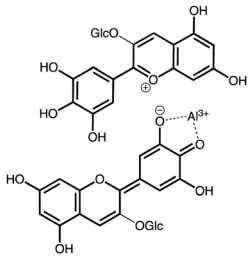

Scheme 8 Representation of the Al(III)–delphinidin complex in acidic ethanol. According to the authors, the flavylium cation stacks on top of the quinoidal base, not next to the quinoidal base anion as shown in this two-dimensional representation.[49]

These results are in apparent contradiction with the job plot reported by the same authors, who identified a 1 : 1 complex.

A complete study of the sepal colour of hydrangea has been carried out by Yoshida and co-workers.[48] These authors were able to measure the vacuolar pH of the sepals and correlate with the concentration of Al^{3+} in the presence of the copigment. The colour is dependent on the pH and Al^{3+} concentration. The appearance of the blue colour is not possible at lower pH values and this is explained by the physical chemistry of the anthocyanin system. The interesting feature is that 1 : 1 equivalent is enough for the appearance of the blue colour in accordance with a very strong complexation constant. The results of Yoshida and co-workers are compatible with an equilibrium between the red flavylium cation and the blue Al^{3+} complex (involving also acylquinic acids in a more complex supramolecular structure).[50] Scheme 9(b) shows a diagram that explains qualitatively the variety of colours observed in *hydrangea* as a function of pH. When the metal is available (requiring acidic soils) it is the pH tuning that controls the appearance of the red, purple and blue colours.

5.5. Supramolecular structures (metaloanthocianins)

The molecular structure that is responsible for the blue colour of *Commelina communis* is a beautiful example of supramolecular chemistry.[25,32] The anthocyanin malonylawobanin, a flavone flavocommelin and Mg(II) cations in a ratio 6 : 6 : 2, respectively, self-assemble as shown in Scheme 10. The crystal

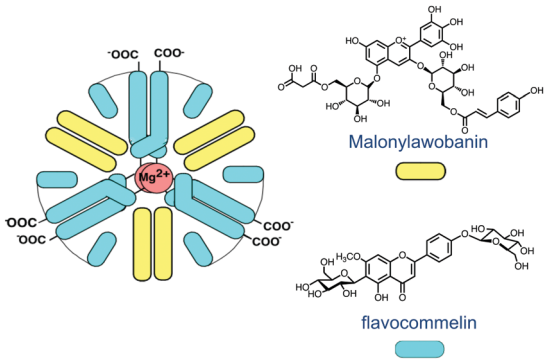

Scheme 10 Sketch illustrating the supramolecular structure that gives colour to *Commelina communis*. By courtesy of Prof. Yoshida.

structure of the reconstructed supramolecule was reported[51] and later the one having Cd(II)[52] and it was revealed that both structures are similar. Shiono *et al.*[53] succeeded in preparing a single crystal from natural *Commelina*, reporting the respective crystal structure, which was identical to the reconstructed one.

The way in which nature was able to fix the blue colour in *Commelina communis* is shown in Scheme 10. An anthocyanin, a flavone and a metal ion in a 6 : 6 : 2 ratio are organized into two parallel planes, each containing 3 anthocyanins, 3 flavones and a metal ion that organizes the space.

The anthocyanin in this beautiful structure bears one acylated unit in both sugars, profits from the intermolecular and intramolecular copigmentation and uses the metal to link ring C to the metal. In other words, all strategies that have been reported above. If we consider that during the evolution of plants the colour systems had a parallel evolution[54] according to our present knowledge this structure is at the top of the evolution.

6. Conclusions

Nature used in ancient plants the multistates of auronidins (liverworts) and 3-deoxyanthocyanins (mosses and ferns) but none of these colour systems were able to get the blue observed in angiosperms or possess a relatively rapid rate of interconversion between the multistate species. Simpler anthocyanins have

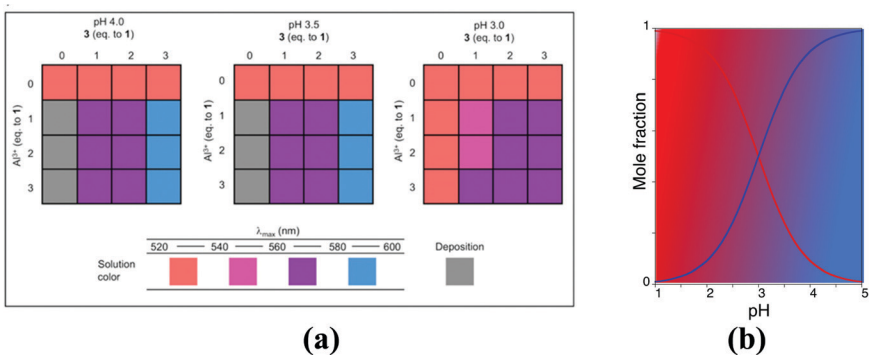

Scheme 9 (a) Box colours as a function pH and Al^{3+} concentration. Adapted from ref. 50, with permission, copyright John Wiley and Sons. (b) The qualitative mole fraction distribution of the red flavylium cation and blue aluminium complex may explain the appearance of the colours.

the colours that angiosperms exhibit but in minor fractions or in unstable species. The appearance of the colour, in particular blue, requires inter or intramolecular interactions respectively with other natural compounds or by means of the acylated sugars. The interaction with metals allows for the reorganization of the space in supramolecular structures that not only complex and stabilize the unstable anionic forms of the anthocyanins bearing a catechol unit but also create the conditions for copigmentation as in the case of the metaloanthocyanins that involve the anionic quinoidal base and the flavone. The use of physical-chemistry tools allows for determination of equilibrium and rate constants leading to quantitative knowledge of the system. The pH dependent mole fraction distributions of the several species in solution are straightforwardly obtained from the equilibrium constants provided that the appropriate models are available. In most cases these systems have been described in a qualitative and phenomenological approach, which while necessary needs to be complemented by the kinetics and thermodynamics of these systems, as reported in this perspective article.

Conflicts of interest

There is no conflict of interest.

Appendix 1A: the complex multistate simplified as a diprotic acid

Let us consider the extension of the equilibrium of anthocyanins and related compounds to the anionic species. The extension to more acid base equilibria is straightforward.

First global acid base equilibrium

$$AH^+ + H_2O \rightleftharpoons A + H_3O^+ \quad K_a \text{ proton transfer} \tag{78}$$

$$AH^+ + 2H_2O \rightleftharpoons B + H_3O^+ \quad K_h \text{ hydration} \tag{79}$$

$$B \rightleftharpoons Cc \quad K_t \text{ tautomerization} \tag{80}$$

$$Cc \rightleftharpoons Ct \quad K_i \text{ isomerization} \tag{81}$$

Second global acid base equilibrium

$$A + H_2O \rightleftharpoons A^- + H_3O^+ \quad K_{A/A^-} \text{ proton transfer} \tag{82}$$

$$B + H_2O \rightleftharpoons B^- + H_3O^+ \quad K_{B/B^-} \text{ proton transfer} \tag{83}$$

$$Cc + H_2O \rightleftharpoons Cc^- + H_3O^+ \quad K_{Cc/Cc^-} \text{ proton transfer} \tag{84}$$

$$Ct + H_2O \rightleftharpoons Ct^- + H_3O^+ \quad K_{Ct/Ct^-} \text{ proton transfer} \tag{85}$$

Inspection of the multistate of reactions shows that, except for the formation of B, Cc and Ct, all the other reactions are proton transfers.

The mole fractions of all the species of the multistate are straightforwardly calculated by a simple mass balance of the species AH^+, by using the equilibrium constants of eqn (78)–(85).

The mass balance gives

$$C_0 = [AH^+] + [A] + [B] + [Cc] + [Ct] + [A^-] + [B^-] + [Cc^-] + [Ct^-] \tag{86}$$

$$C_0 = [AH^+]\left(1 + \frac{K_a}{[H^+]} + \frac{K_h}{[H^+]} + \frac{K_hK_t}{[H^+]} + \frac{K_hK_tK_i}{[H^+]} + \frac{K_{A/A^-}K_a}{[H^+]^2} + \frac{K_{B/B^-}K_h}{[H^+]^2} + \frac{K_{Cc/Cc^-}K_hK_t}{[H^+]^2} + \frac{K_{Ct/Ct^-}K_hK_tK_i}{[H^+]^2}\right) \tag{87}$$

From eqn (87) the mole fraction distribution of AH^+ can be calculated, eqn (88)

$$X_{AH^+} = \frac{[AH^+]}{C_0} = \frac{[H^+]^2}{D} \tag{88}$$

where

$$D = [H^+]^2 + (K_a + K_h + K_hK_t + K_hK_tK_i)[H^+] + \left(K_{A/A^-}K_a + K_{B/B^-}K_h + K_{Cc/Cc^-}K_hK_t + K_{Ct/Ct^-}K_hK_tK_i\right)$$

By analogy with the general equation for a di-protic acid where K_a' and K_a'' are the first and second acidity constants, the mole fraction of the fully protonated form is given by eqn (89)

$$X_{AH^+} = \frac{[H^+]^2}{[H^+]^2 + K_a'[H^+] + K_a'K_a''} \tag{89}$$

with

$$K_a' = K_a + K_h + K_hK_t + K_hK_tK_i \tag{90}$$

$$K_a'K_a'' = K_{A/A^-}K_a + K_{B/B^-}K_h + K_{Cc/Cc^-}K_hK_t + K_{Ct/Ct^-}K_hK_tK_i \tag{91}$$

The complex equilibria from eqn (78)–(85) can thus be summarized in eqn (92) and (93)

$$AH^+ + H_2O \rightleftharpoons CB + H_3O^+ \quad K_a' \tag{92}$$

$$CB + H_2O \rightleftharpoons CB^- + H_3O^+ \quad K_a'' \tag{93}$$

where

$$[CB] = [A] + [B] + [Cc] + [Ct] \tag{94}$$

$$[CB^-] = [A^-] + [B^-] + [Cc^-] + [Ct^-] \tag{95}$$

with K_a' defined by eqn (90) and (92) and K_a'' by eqn (93) and (96).

$$K_a'' = \frac{K_{A/A^-}K_a + K_{B/B^-}K_h + K_{Cc/Cc^-}K_hK_t + K_{Ct/Ct^-}K_hK_tK_i}{K_a'} \tag{96}$$

The mole fraction of the remaining species is now easy to obtain from eqn (97)–(104)

$$X_A = \frac{K_a[H^+]}{[H^+]^2 + K_a'[H^+] + K_a'K_a''} = \frac{K_a[H^+]}{D} \tag{97}$$

$$X_B = \frac{K_h[H^+]}{D} \tag{98}$$

$$X_{Cc} = \frac{K_hK_t[H^+]}{D} \tag{99}$$

$$X_{Ct} = \frac{K_h K_t K_i [H^+]}{D} \quad (100)$$

$$X_{A^-} = \frac{K_a K_{A/A^-}}{D} \quad (101)$$

$$X_{B^-} = \frac{K_h K_{B/B^-}}{D} \quad (102)$$

$$X_{Cc^-} = \frac{K_h K_t K_{Cc/Cc^-}}{D} \quad (103)$$

$$X_{Ct^-} = \frac{K_h K_t K_i K_{Ct/Ct^-}}{D} \quad (104)$$

On the other hand, eqn (92) and (93) show that the system behaves as a diprotic acid with constants K_a' and K_a''. The respective mole fractions are given by eqn (105)–(107)

$$X_{AH^+} = \frac{[H^+]^2}{D} \qquad D = [H^+]^2 + K_a'[H^+] + K_a' K_a'' \quad (105)$$

$$X_{CB} = \frac{K_a'[H^+]}{D} \quad (106)$$

$$X_{CB^-} = \frac{K_a' K_a'}{D} \quad (107)$$

Pseudo equilibrium

All equations described above can be applied at the pseudo-equilibrium. The pseudo equilibrium is reached when the isomerization constant is by far the slowest step of the kinetics towards the equilibrium.

$$AH^+ + H_2O \rightleftharpoons CB^\wedge + H_3O^+ \quad K^\wedge_a \quad (108)$$

$$CB^\wedge + H_2O \rightleftharpoons CB^{\wedge -} + H_3O^+ \quad K^{\wedge\wedge}_a \quad (109)$$

where

$$[CB^\wedge] = [A] + [B] + [Cc] + [Ct] \quad (110)$$

$$[CB^{\wedge -}] = [A^-] + [B^-] + [Cc^-] + [Ct^-] \quad (111)$$

The mole fractions of the pseudo equilibrium are given by the same expression as the equilibrium making $K_i = 0$ with

$$K^\wedge_a = K_a + K_h + K_h K_t \quad (112)$$

$$K^\wedge_a K^{\wedge\wedge}_a = K_{A/A^-} K_a + K_{B/B^-} K_h + K_{Cc/Cc^-} K_h K_t \quad (113)$$

and by consequence

$$K^{\wedge\wedge}_a = \frac{K_{A/A^-} K_a + K_{B/B^-} K_h + K_{Cc/Cc^-} K_h K_t}{K^\wedge_a} \quad (114)$$

The mole fraction of the global diprotic acid at the pseudo-equilibrium is given by

$$X_{AH^+} = \frac{[H^+]^2}{D^\wedge} \quad D^\wedge = [H^+]^2 + K^\wedge_a [H^+] + K^\wedge_a K^{\wedge\wedge}_a \quad (115)$$

$$X_{CB^\wedge} = \frac{K^\wedge_a [H^+]}{D^\wedge} \quad (116)$$

$$X_{CB^{\wedge -}} = \frac{K^\wedge_a K^{\wedge\wedge}_a}{D^\wedge} \quad (117)$$

Appendix 1B: reverse pH jumps

As shown in the main text, at the pseudo equilibrium (*mutatis mutandis* for the equilibrium) the normalized mole fraction distribution of the species A, B and Cc can be calculated through reverse pH jumps. Fig. 5 of the main text shows a simulation of these mole fractions for several pH values. In other words, $CB^\wedge$ and $CB^{\wedge -}$ can be decomposed into their components. This means that for example the mole fraction of CB can be written as follows,

$$X_{CB} = \frac{K^\wedge_a [H^+]}{D^\wedge} = a_0 \frac{K^\wedge_a [H^+]}{D^\wedge} + b_0 \frac{K^\wedge_a [H^+]}{D^\wedge} + c_0 \frac{K^\wedge_a [H^+]}{D^\wedge} \quad (118)$$

where a_0, b_0 and c_0 are the normalized mole fractions respectively of A, B and Cc

$$a_0 + b_0 + c_0 = 1 \quad (119)$$

The same for $CB^{\wedge -}$

$$X_{CB^{\wedge -}} = \frac{K^\wedge_a K^{\wedge\wedge}_a [H^+]}{D^\wedge} = a_1 \frac{K^\wedge_a K^{\wedge\wedge}_a [H^+]}{D^\wedge} + b_1 \frac{K^\wedge_a K^{\wedge\wedge}_a [H^+]}{D^\wedge} + c_1 \frac{K^\wedge_a K^{\wedge\wedge}_a [H^+]}{D^\wedge} \quad (120)$$

$$a_1 + b_1 + c_1 = 1 \quad (121)$$

The normalized mole fractions of each species and the respective ionized forms can be written

$$X_A + X_{A^-} = a_0 \frac{K^\wedge_a [H^+]}{D^\wedge} + a_1 \frac{K^\wedge_a K^{\wedge\wedge}_a}{D^\wedge} \quad (122)$$

$$X_B + X_{B^-} = b_0 \frac{K^\wedge_a [H^+]}{D^\wedge} + b_1 \frac{K^\wedge_a K^{\wedge\wedge}_a}{D^\wedge} \quad (123)$$

$$X_{Cc} + X_{Cc^-} = c_0 \frac{K^\wedge_a [H^+]}{D^\wedge} + c_1 \frac{K^\wedge_a K^{\wedge\wedge}_a}{D^\wedge} \quad (124)$$

The mole fractions calculated in Appendix 1A can be re-written as follows

$$X_A + X_{A^-} = \frac{K_a [H^+] + K_{A/A^-} K_a}{[H^+]^2 + K^\wedge a [H^+] + K^\wedge_a K^{\wedge\wedge}_a} = \frac{K_a [H^+] + K_{A/A^-} K_a}{D^\wedge} \quad (125)$$

$$X_B + X_{B^-} = \frac{K_h [H^+] + K_{B/B^-} K_h}{D^\wedge} \quad (126)$$

$$X_{Cc} + X_{Cc^-} = \frac{K_h K_t [H^+] + K_{Cc/Cc^-} K_h K_t}{D^\wedge} \quad (127)$$

Comparing eqn (122)–(124) with eqn (125)–(127)

$$K_a = a_0 K^\wedge_a; \quad K_{A/A^-} K_a = a_1 K^\wedge_a K^{\wedge\wedge}_a;$$
$$K_{A^-/A^{2-}} K_{A/A^-} K_a = a_2 K^{\wedge\wedge}_a K^{\wedge\wedge}_a K^{\wedge\wedge\wedge}_a$$
$$K_h = b_0 K^\wedge_a; \quad K_{B/B^-} K_h = b_1 K^\wedge_a K^{\wedge\wedge}_a;$$
$$K_{B^-/B^{2-}} K_{B/B^-} K_h = b_2 K^\wedge_a K^{\wedge\wedge}_a K K^{\wedge\wedge\wedge}_a$$
$$K_h K_t = c_0 K^\wedge_a; \quad K_{Cc/CC^-} K_h K_t = c_1 K^\wedge_a K^{\wedge\wedge}_a;$$
$$K_{Cc^-/Cc^{2-}} K_{Cc/Cc^-} K_h K_t = c_2 K^\wedge_a K^{\wedge\wedge}_a K K^{\wedge\wedge\wedge}_a$$

This permits one to calculate all equilibrium constants, since $K^\wedge_a$, $K^{\wedge\wedge}_a$ and $K^{\wedge\wedge\wedge}_a$ are calculated from the pseudo-equilibrated absorption spectra. At any wavelength the absorption as a function of pH exhibits 2 inflection points corresponding to the two pK_as.

Appendix 2: copigmentation constants by reverse pH jumps (stopped flow)

Considering the flavylium cation and the neutral species

$$AH^+ + H_2O \rightleftharpoons A + H_3O^+ \quad K_a \text{proton transfer} \quad (128)$$
$$AH^+ + H_2O \rightleftharpoons B + H_3O^+ \quad K_h \text{ hydration} \quad (129)$$
$$B \rightleftharpoons Cc \quad K_t \text{ tautomerization} \quad (130)$$

This equation is reduced to

$$AH^+ + H_2O \rightleftharpoons CB^\wedge + H_3O^+ \quad K^\wedge_a \text{ proton transfer} \quad (131)$$

$$[CB^\wedge] = [A] + [B] + [Cc]$$
$$K^\wedge_a = K_a + K_h + K_h K_t \quad (132)$$

Considering the 1 : 1 complexation with neutral species

$$AH^+ + CP \rightleftharpoons AH^+CP \quad K_{AH+CP} \text{ complexation} \quad (133)$$
$$A + CP \rightleftharpoons ACP \quad K_{ACP} \text{ complexation} \quad (134)$$
$$B + CP \rightleftharpoons BCP \quad K_{BCP} \text{ complexation} \quad (135)$$
$$Cc + CP \rightleftharpoons CcCP \quad K_{CcCP} \text{ complexation} \quad (136)$$

This complex set of equations can be reduced to eqn (131) and (137)

$$CB^\wedge + CP \rightleftharpoons CB^\wedge CP \quad K_{CBCP} \text{ complexation} \quad (137)$$

$$[CB^\wedge CP] = [ACP] + [BCP] + [CcCP]$$
$$K_{CB^\wedge CP} = \frac{[CB^\wedge CP]}{[CB^\wedge][CP]} = \frac{[ACP] + [BCP] + [CcCP]}{[A][CP] + [B][CP] + [Cc][CP]} \quad (138)$$

Simplifying

$$K_{CB^\wedge CP} = \frac{[CB^\wedge CP]}{[CB^\wedge][CP]} = \frac{K_{ACP}K_a + K_{BCP}K_h + K_{CcCP}K_h K_t}{K^\wedge_a} \quad (139)$$

Considering the mono-ionized species, those that still have some importance in anthocyanins (the higher ionized species are not stable)

$$A + H_2O \rightleftharpoons A^- + H_3O^+ \quad K_{A/A^-} \text{ proton transfer} \quad (140)$$
$$B + H_2O \rightleftharpoons B^- + H_3O^+ \quad K_{B/B^-} \text{ proton transfer} \quad (141)$$
$$Cc + H_2O \rightleftharpoons Cc^- + H_3O^+ \quad K_{Cc/cc^-} \text{ proton transfer} \quad (142)$$

Eqn (140)–(142) are reduced to eqn (143)

$$CB^\wedge + H_2O \rightleftharpoons CB^{\wedge -} + H_3O^+ \quad K_{CB^\wedge/CB^{\wedge -}} \text{ proton transfer} \quad (143)$$

This constant can be written as in eqn (144)

$$K_{CB^\wedge/CB^{\wedge -}} = \frac{([A^-] + [B^-] + [Cc^-])[H^+]}{[CB^\wedge]} = \frac{K_{A/A^-}K_a + K_{B/B^-}K_h + K_{Cc/Cc^-}K_h K_t}{K^\wedge_a} \quad (144)$$

Regarding the complexation of the ionized species

$$A^- + CP \rightleftharpoons A^-CP \quad K_{ACP} \text{ complexation} \quad (145)$$
$$B^- + CP \rightleftharpoons B^-CP \quad K_{BCP} \text{ complexation} \quad (146)$$
$$Cc^- + CP \rightleftharpoons Cc^-CP \quad K_{CcCP} \text{ complexation} \quad (147)$$

can be reduced to

$$CB^{\wedge -} + CP \rightleftharpoons CB^{\wedge -}CP \quad K_{(CB^\wedge - CP)} \quad (148)$$

$$K_{CB^{\wedge -}CP} = \frac{[CB^{\wedge -}CP]}{[CB^{\wedge -}][CP]} = \frac{[A^-CP] + [B^-CP] + [Cc^-CP]}{[A^-][CP] + [B^-][CP] + [Cc^-][CP]} \quad (149)$$

giving

$$K_{CB^\wedge - CP} = \frac{K_{ACP/ACP-}K_{A/A-}K_a + K_{BCP/BCP-}K_{B/B-}K_h + K_{CcCP/CcCP-}K_{Cc/Cc-}K_h K_t}{K_{CB^\wedge/CB^\wedge -}K^\wedge_a} \quad (150)$$

Summarizing, the complex set of equations can be dramatically simplified to a diprotic acid where three species can be involved in complexation. The system is defined by two acid base constants given by eqn (139) and (144), respectively, $AH^+/CB^\wedge$ and $CB^\wedge/CB^{\wedge -}$, and three complexation constants eqn (133), (139) and (150), respectively, with the flavylium cation, $CB^\wedge$ and $CB^{\wedge -}$.

In order to get the mole fractions of all species mass balance must be found

$$C_0 = [AH^+] + [A] + [B] + [Cc] + [A^-] + [B^-] + [Cc^-] + [AH^+CP] + [ACP] + [BCP] + [CcCP] + [A^-CP] + [B^-CP] + [Cc^-CP] \quad (151)$$

From the set of equations above all species can be written in terms of AH^+

$$C_0 = [AH^+]\left(1+\frac{K_a}{[H^+]}+\frac{K_h}{[H^+]}+\frac{K_hK_t}{[H^+]}+\frac{K_{A/A^-}K_a}{[H^+]^2}+\frac{K_{B/B^-}K_h}{[H^+]^2}+\frac{K_{Cc/CC^-}K_hK_t}{[H^+]^2}+K_{AH+CP}[CP]+K_{ACP}\frac{K_a}{[H^+]}[CP]+K_{BCP}\frac{K_h}{[H^+]}[CP]+K_{CcCP}\frac{K_hK_t}{[H^+]}[CP]+\frac{K_{ACP/ACP^-}K_{ACP}K_a}{[H^+]^2}[CP]+\frac{K_{BCP/BCP^-}K_{BCP}K_h}{[H^+]^2}[CP]+\frac{K_{CcCP/CcCP^-}K_{CcCP}K_hK_t}{[H^+]^2}[CP]\right) \quad (152)$$

$$C_0 = [AH^+]\left(1+K_{AH+CP}[CP]+\frac{K_a+K_h+K_hK_t+K_{ACP}K_a[CP]+K_{BCP}K_h[CP]+K_{CcCP}K_hK_t[CP]}{[H^+]}+\frac{K_{A/A^-}K_a+K_{B/B^-}K_h+K_{Cc/CC^-}K_hK_t+\left(K_{ACP/ACP^-}K_{ACP}K_a+K_{BCP/BCP^-}K_{BCP}K_h+K_{CcCP/CcCP^-}K_{CcCP}K_hK_t\right)[CP]}{[H^+]^2}\right) \quad (153)$$

or simplifying

$$C_0 = [AH^+]\left(1+K_{AH+CP}[CP]+\frac{K^{\wedge}_a+K_1[CP]}{[H^+]}+\frac{K_2+K_3[CP]}{[H^+]^2}\right) \quad (154)$$

with

$$\begin{aligned} K^{\wedge}_a &= K_a+K_h+K_hK_t \\ K_1 &= K_{ACP}K_a+K_{BCP}K_h+K_{CcCP}K_hK_t \\ K_2 &= K_{A/A^-}K_a+K_{B/B^-}K_h+K_{Cc/CC^-}K_hK_t \\ K_3 &= K_{ACP/ACP^-}K_{ACP}K_a+K_{BCP/BCP^-}K_{BCP}K_h \\ &\quad +K_{CcCP/CcCP^-}K_{CcCP}K_hK_t \end{aligned} \quad (155)$$

The mole fraction of AH^+ can now be written

$$\begin{aligned} X_{AH^+} &= \frac{[AH^+]}{C_0} \\ &= \frac{1}{(1+K_{AH+CP}[CP])+\frac{K^{\wedge}_a+K_1[CP]}{[H^+]}+\frac{K_2+K_3[CP]}{[H^+]^2}} \\ &= \frac{\frac{1}{(1+K_{AH+CP}[CP])}[H^+]^2}{[H^+]^2+\frac{K^{\wedge}_a+K_1[CP]}{(1+K_{AH+CP}[CP])}[H^+]+\frac{K_2+K_3[CP]}{(1+K_{AH+CP}[CP])}} \end{aligned} \quad (156)$$

$$\begin{aligned} X_{AH+CP} &= \frac{[AH^+CP]}{C_0} \\ &= \frac{\frac{K_{AH+CP}[CP]}{(1+K_{AH+CP}[CP])}[H^+]^2}{[H^+]^2+\frac{K^{\wedge}_a+K_1[CP]}{(1+K_{AH+CP}[CP])}[H^+]+\frac{K_2+K_3[CP]}{(1+K_{AH+CP}[CP])}} \end{aligned} \quad (157)$$

The sum of both mole fractions

$$X_{AH^+}+X_{AH+CP} = \frac{[H^+]^2}{[H^+]^2+K^{\wedge}_{a(CP)}[H^+]+K^{\wedge}_{a(CP)}K^{\wedge\wedge}_{a(CP)}} \quad (158)$$

The values $K^{\wedge}_{a(CP)}$ and $K^{\wedge\wedge}_{a(CP)}$ are obtained experimentally, corresponding to the inflection points when the absorbance is represented as a function of pH, as well as in the experiments of the reverse pH jumps. The constant K_{AH+CP} is calculated by representing the absorption of the flavylium cation at pH = 1 as a function of the co-pigment concentration.

The mole fraction of A and ACP and their ionized species is obtained from the contributions

$$\begin{aligned} &X_A+X_{ACP}+X_{A^-}+X_{ACP^-} \\ &= \frac{\frac{K_a+A_{ACP}K_a[CP]}{(1+K_{AH+CP}[CP])}[H^+]+\frac{K_{A/A^-}K_a+K_{ACP/ACP^-}K_{ACP}K_a[CP]}{(1+K_{AH+CP}[CP])}}{[H^+]^2+K^{\wedge}_{a(CP)}[H^+]+K^{\wedge}_{a(CP)}K^{\wedge\wedge}_{a(CP)}} \end{aligned} \quad (159)$$

$$\begin{aligned} K^{\wedge}_a &= K_a \\ K_1 &= K_{ACP}K_a \\ K_2 &= K_{A/A^-}K_a \\ K_3 &= K_{ACP/ACP^-}K_{ACP}K_a \end{aligned} \quad (160)$$

Identically for the hemiketal and *cis*-chalcones

$$\begin{aligned} &X_B+X_{BCP}+X_{B^-}+X_{B^-CP} \\ &= \frac{(K_h+K_{BCP}K_h[CP])[H^+]+K_{B/B^-}K_h+K_{BCP/BCP^-}K_{BCP}K_h[CP]}{(1+K_{AH^+CP}[CP])} \\ &\quad [H^+]^2+K^{\wedge}_{a(CP)}[H^+]+K^{\wedge}_{a(CP)}K^{\wedge\wedge}_{a(CP)} \end{aligned} \quad (161)$$

On the other hand, the reverse pH jumps in the presence of a

$$\begin{aligned} &X_{Cc}+X_{CcCP}+X_{Cc^-}+X_{Cc^-CP} \\ &= \frac{(K_hK_t+K_{CcCP}K_hK_t[CP])[H^+]+K_{Cc/Cc^-}K_hK_t+K_{CcCP/CcCP^-}K_{CcCP}K_hK_t[CP]}{(1+K_{AH^+CP}[CP])} \\ &\quad [H^+]^2+K^{\wedge}_{a(CP)}[H^+]+K^{\wedge}_{a(CP)}K^{\wedge\wedge}_{a(CP)} \end{aligned} \quad (162)$$

co-pigment can be written for AH^+, A, A^- and their respective co-pigments (in reverse pH jumps all these species appear as the initial absorption), as follows:

$$X_{AH^+} + X_{AH+CP} + X_A + X_{ACP} + X_{A^-} + X_{A^-CP} = \frac{[H^+]^2 + a_{0(CP)}K^{\wedge}_{a(CP)}[H^+] + a_{1(CP)}K^{\wedge}_{a(CP)}K^{\wedge\wedge}_{a(CP)}}{[H^+]^2 + K^{\wedge}_{a(CP)}[H^+] + K^{\wedge}_{a(CP)}K^{\wedge\wedge}_{a(CP)}} \quad (163)$$

where $a_{0(CP)}$ and $a_{1(CP)}$ are respectively the mole fraction of A plus ACP and A^- plus ACP^-.

Consequently

$$X_{Ct} + X_{CtCP} + X_{Ct^-} + X_{Ct^-CP} = \frac{(K_hK_tK_i + K_{CtCP}K_hK_tK_i[CP])[H^+] + K_{Ct/Ct^-}K_hK_tK_i + K_{CtCP/CtCP^-}K_{CtCP}K_hK_tK_i[CP]}{(1 + K_{AH^+CP}[CP])} \Big/ \frac{}{[H^+]^2 + K'_{a(CP)}[H^+] + K'_{a(CP)}K''_{a(CP)}} \quad (173)$$

$$a_{0(CP)}K^{\wedge}_{a(CP)} = \frac{K_a + A_{ACP}K_a[CP]}{(1 + K_{AH+CP}[CP])} \quad (164)$$

$$a_{1(CP)}K^{\wedge}_{a(CP)}K^{\wedge\wedge}_{a(CP)} = \frac{K_{ACP/ACP^-}K_{ACP}K_a}{1 + K_{AH+CP}[CP]} \quad (165)$$

Proceeding identically for the other species

$$X_B + X_{BCP} + X_{B^-} + X_{B^-CP} = \frac{b_{0(CP)}K^{\wedge}_{a(CP)}[H^+] + b_{1(CP)}K^{\wedge}_{a(CP)}K^{\wedge\wedge}_{a(CP)}}{[H^+]^2 + K^{\wedge}_{a(CP)}[H^+] + K^{\wedge}_{a(CP)}K^{\wedge\wedge}_{a(CP)}} \quad (166)$$

$$X_{Cc} + X_{CcCP} + X_{Cc^-} + X_{Cc^-CP} = \frac{c_{0(CP)}K^{\wedge}_{a(CP)}[H^+] + c_{1(CP)}K^{\wedge}_{a(CP)}K^{\wedge\wedge}_{a(CP)}}{[H^+]^2 + K^{\wedge}_{a(CP)}[H^+] + K^{\wedge}_{a(CP)}K^{\wedge\wedge}_{a(CP)}} \quad (167)$$

$$b_{0(CP)}K^{\wedge}_{a(CP)} = \frac{K_h + A_{BCP}K_h[CP]}{(1 + K_{AH+CP}[CP])} \quad (168)$$

$$b_{1(CP)}K^{\wedge}_{a(CP)}K^{\wedge\wedge}_{a(CP)} = \frac{K_{BCP/BCP^-}K_{BCP}K_h}{1 + K_{AH+CP}[CP]} \quad (169)$$

$$c_{0(CP)}K^{\wedge}_{a(CP)} = \frac{K_hK_t + K_{CcCP}K_hK_t[CP]}{(1 + K_{AH+CP}[CP])} \quad (170)$$

$$c_{1(CP)}K^{\wedge}_{a(CP)}K^{\wedge\wedge}_{a(CP)} = \frac{K_{CcCP/CCCP^-}K_{CcCP}K_hK_t}{1 + K_{AH+CP}[CP]} \quad (171)$$

Summarizing, eqn (164), eqn (166) and eqn (168) give respectively K_{ACP}, K_{BCP} and K_{CcCP}.

On the other hand, eqn (165), eqn (167) and eqn (169) give respectively the ionization constant of the complexes K_{ACP/ACP^-}, K_{ABCP/BCP^-}, and $K_{CcCP/CcCP^-}$.

It is easy to prove that

$$K_{ACP/ACP^-} = \frac{K_{ACP^-}}{K_{ACP}}K_{A/A^-};$$

$$K_{BCP/BCP^-} = \frac{K_{BCP^-}}{K_{BCP}}K_{B/B^-}; \quad (172)$$

$$K_{CcCP/CcCP^-} = \frac{K_{CcCP^-}}{K_{CcCP}}K_{Cc/Cc^-}$$

When the equilibrium is considered the contribution of *trans*-chalcones should be added

$$X_{Ct} + X_{CtCP} + X_{Ct^-} + X_{Ct^-CP} = \frac{d_{0(CP)}K'_{a(CP)}[H^+] + d_{1(CP)}K'_{a(CP)}K''_{a(CP)}}{[H^+]^2 + K'_{a(CP)}[H^+] + K'_{a(CP)}K''_{a(CP)}} \quad (174)$$

$$d_{0(CP)}K'_{a(CP)} = \frac{K_hK_tK_i + K_{CtCP}K_hK_tK_i[CP]}{(1 + K_{AH+CP}[CP])} \quad (175)$$

$$d_{1(CP)}K'_{a(CP)}K''_{a(CP)} = \frac{K_{CtCP/CtCP^-}K_{CcCP}K_hK_tK_i}{1 + K_{AH+CP}[CP]} \quad (176)$$

Comparing eqn (173) with eqn (175)

$$d_{0(CP)}K'_{a(CP)} = \frac{K_hK_tK_i + K_{CtCP}K_hK_tK_i[CP]}{(1 + K_{AH+CP}[CP])} \quad (177)$$

$$d_{1(CP)}K'_{a(CP)}K''_{a(CP)} = \frac{K_{CtCP/CtCP^-}K_{CtCP}K_hK_tK_i}{1 + K_{AH+CP}[CP]} \quad (178)$$

and

$$K_{CtCP/CtCP^-} = \frac{K_{CtCP^-}}{K_{CtCP}}K_{Ct/Ct^-} \quad (179)$$

Appendix 3: complexation with aluminium

Theory

The system can be accounted for by means of eqn (180)–(182).

$$AH^+ + H_2O \rightleftharpoons A + H_3O^+ \quad K_a \text{ proton transfer} \quad (180)$$

$$A + H_2O \rightleftharpoons A^- + H_3O^+ \quad K_{A/A^-} \text{ proton transfer} \quad (181)$$

$$A^- + Al^{3+} \rightleftharpoons Al^{3+}A^-$$
$$K_{CP(A^-)} = \frac{[Al^{3+}A^-]}{[Al^{3+}][A^-]} \text{ complexation} \quad (182)$$

The mass balance for the metal is given by eqn (183).

$$C_{0(\mathrm{Al})} = [\mathrm{Al}^{3+}]\left(1+\frac{K_{a1}}{[\mathrm{H}^+]}+\frac{K_{a1}K_{a2}}{[\mathrm{H}^+]^2}+\frac{K_{a1}K_{a2}K_{a3}}{[\mathrm{H}^+]^3} + \frac{K_{a1}K_{a2}K_{a3}K_{a4}}{[\mathrm{H}^+]^4}+K_{\mathrm{CP(A^-)}}\frac{K_{\mathrm{A/A^-}}K_a}{[\mathrm{H}^+]^2}[\mathrm{AH}^+]\right) \quad (183)$$

Introducing the parameter α

$$\alpha = 1+\frac{K_{a1}}{[\mathrm{H}^+]}+\frac{K_{a1}K_{a2}}{[\mathrm{H}^+]^2}+\frac{K_{a1}K_{a2}K_{a3}}{[\mathrm{H}^+]^3}+\frac{K_{a1}K_{a2}K_{a3}K_{a4}}{[\mathrm{H}^+]^4} \quad (184)$$

The mass balance of the metal can be re-written as in eqn (185).

$$C_{0(\mathrm{Al})} = [\mathrm{Al}^{3+}]\left(\alpha+K_{\mathrm{CP(A^-)}}\frac{K_{\mathrm{A/A^-}}K_a}{[\mathrm{H}^+]^2}[\mathrm{AH}^+]\right) \quad (185)$$

The mass balance of the anthocyanin model is given by eqn (186).

$$C_{0(\mathrm{antho})} = [\mathrm{AH}^+]\left(1+\frac{K_a}{[\mathrm{H}^+]}+\frac{K_{\mathrm{A/A^-}}K_a}{[\mathrm{H}^+]^2}+K_{\mathrm{CP(A^-)}}\frac{K_{\mathrm{A/A^-}}K_a}{[\mathrm{H}^+]^2}[\mathrm{Al}^{3+}]\right) \quad (186)$$

Introducing the parameter β,

$$\beta = 1+\frac{K_a}{[\mathrm{H}^+]}+\frac{K_{\mathrm{A/A^-}}K_a}{[\mathrm{H}^+]^2} \quad (187)$$

$$C_{0(\mathrm{antho})} = [\mathrm{AH}^+]\left(\beta+K_{\mathrm{CP(A^-)}}\frac{K_{\mathrm{A/A^-}}K_a}{[\mathrm{H}^+]^2}[\mathrm{Al}^{3+}]\right) \quad (188)$$

Introducing γ

$$\gamma = K_{\mathrm{CP(A^-)}}\frac{K_{\mathrm{A/A^-}}K_a}{[\mathrm{H}^+]^2} \quad (189)$$

Two equations and two unknowns are obtained.

$$[\mathrm{Al}^{3+}] = \frac{C_{0(\mathrm{Al})}}{\alpha+\gamma[\mathrm{AH}^+]} \quad (190)$$

$$[\mathrm{AH}^+] = \frac{C_{0(\mathrm{antho})}}{(\beta+\gamma[\mathrm{Al}^{3+}])} \quad (191)$$

Substituting in eqn (191) the value of $[\mathrm{Al}^{3+}]$, eqn (190)

$$[\mathrm{AH}^+] = \frac{C_{0(\mathrm{antho})}}{\left(\beta+\gamma\frac{C_{0(\mathrm{Al})}}{\alpha+\gamma[\mathrm{AH}^+]}\right)} \quad (192)$$

A quadratic equation is obtained, eqn (193)

$$\gamma\beta[\mathrm{AH}^+]^2 + (\alpha\beta + \gamma C_{0(\mathrm{Al})} - \gamma C_{0(\mathrm{antho})})[\mathrm{AH}^+] - \alpha C_{0(\mathrm{antho})} = 0 \quad (193)$$

All parameters in eqn (193) except $K_{\mathrm{CP(A^-)}}$ are known and a fitting of the experimental data only needs to adjust this constant.

The variation of the absorbance at longer wavelengths *versus* pH is accounted for by means of eqn (194)

$$A_\lambda = \varepsilon_{\mathrm{AH^+}}[\mathrm{AH}^+] + \varepsilon_{\mathrm{A}}[\mathrm{A}] + \varepsilon_{\mathrm{A^-}}[\mathrm{A}^-] + \varepsilon_{\mathrm{Al^{3+}A^-}}[\mathrm{Al_3A}^-] \quad (194)$$

which can be written as in eqn (195)

$$A_\lambda = c_1\chi_{\mathrm{AH^+}} + c_2\chi_{\mathrm{A}} + c_3\chi_{\mathrm{A^-}} + c_4\chi_{\mathrm{Al^{3+}A^-}}$$
$$c_1 = \varepsilon_{\mathrm{AH^+}}C_{0(\mathrm{Antho})}; \quad c_2 = \varepsilon_{\mathrm{A}}C_{0(\mathrm{Antho})}; \quad (195)$$
$$c_3 = \varepsilon_{\mathrm{A^-}}C_{0(\mathrm{Antho})}; \quad c_4 = \varepsilon_{\mathrm{AH^+A^-}}C_{0(\mathrm{Antho})}$$

where ε stands for the mole absorption coefficient of the flavylium cation, quinoidal base, anionic quinoidal base and the 1 : 1 complex $\mathrm{Al^{3+}A^-}$, the species that absorb light at longer wavelengths, and χ is the respective mole fraction. (In the case of very high complexation constants the mole fractions of A and $\mathrm{A^-}$ can be neglected.)

The fitting of the data reported in Fig. 7 of the main text was achieved by means of eqn (195) using the quadratic eqn (193), to calculate the free flavylium cation and metal, and consequently all the species absorbing in the visible, for the parameters c_1 = 0.398, c_2 = c_3 = 0, c_4 = 0.05, at 430 nm, and K_{CP} = 2×10^8 $\mathrm{M^{-1}}$ and for a total concentration of the compound of 5×10^{-5} M, independently of the metal concentration in excess.

Simplification of the system

It is straightforward to prove that when the complexation constant is very high the mole fraction of the free A and $\mathrm{A^-}$ can be neglected (as in the case of catechol described above) and the mass balance becomes

$$C_0 = [\mathrm{AH}^+] + [\mathrm{A^-Al^{3+}}] = [\mathrm{AH}^+]\left(1+\frac{K_aK_{\mathrm{A/A^-}}K_{\mathrm{CP}}[\mathrm{Al}^{3+}]}{[\mathrm{H}^+]^2}\right) \quad (196)$$

$$\chi_{\mathrm{AH^+}} = \frac{[\mathrm{H}^+]^2}{([\mathrm{H}^+]^2 + K_aK_{\mathrm{A/A^-}}K_{\mathrm{CP}}[\mathrm{Al}^{3+}])}; \quad \chi_{\mathrm{A^-Al^{3+}}} = \frac{K_aK_{\mathrm{A/A^-}}K_{\mathrm{CP}}[\mathrm{Al}^{3+}]}{([\mathrm{H}^+]^2 + K_aK_{\mathrm{A/A^-}}K_{\mathrm{CP}}[\mathrm{Al}^{3+}])} \quad (197)$$

$$A_\lambda = c_0\chi_{\mathrm{AH^+}} + c_3\chi_{\mathrm{A^-Al^{3+}}} \quad (198)$$

The fitting reported in Fig. 7 of the main text was achieved for $\mathrm{p}K_a$ = 4, $\mathrm{p}K_{\mathrm{A/A^-}}$ = 6.8 and K_{CP} = 2×10^8 $\mathrm{M^{-1}}$, Table 4, and c_0 = 0.385 and c_3 = 0.05, the same parameters reported above. This approximation was previously reported.[47]

Acknowledgements

This work was supported by the Associated Laboratory for Sustainable Chemistry, Clean Processes and Technologies LAQV through the national funds from UIDB/50006/2020 and UIDP/50006/2020 and by AgriFood XXI I&D&I project (NORTE-01-0145-FEDER-000041) cofinanced by European Regional Development Fund (ERDF), through the NORTE 2020 (Programa Operacional Regional do Norte 2014/2020). J. A. and A. S. and J. M. gratefully acknowledge their doctoral grants from FCT: SFRH/BD/139709/2018 and 2020.07313.BD, respectively, and J. M. CONACyT

(MEX/Ref. 288188). J. O. and N. B. would like to thank FCT respectively for contract (IF/00225/2015) and CEECIND/00466/2017.

References

1 J. Guo and M. Wang, *Plant Growth Reg.*, 2010, **62**, 1–8.
2 H. Zhu, T. J. Zhang, J. Zheng, X. D. Huang, Z. C. Yu, C. L. Peng and W. S. Chow, *Photosynthetica*, 2018, **56**, 445–454.
3 N. U. Ahmed, J. I. Park, H. J. Jung, T. J. Yang, Y. Hur and I. S. Nou, *Gene*, 2014, **550**, 46–55.
4 L. Chalker-Scott, *Photochem. Photobiol.*, 1999, **70**, 1–9.
5 J. B. Harborne and C. A. Williams, *Phytochemistry*, 2000, **55**, 481–504.
6 M. E. Hoballah, T. Gübitz, J. Stuurman, L. Broger, M. Barone, T. Mandel, A. Dell'Olivo, M. Arnold and C. Kuhlemeier, *Plant Cell*, 2007, **19**, 779–790.
7 J. Tilbrook and S. D. Tyerman, *Funct. Plant Biol.*, 2008, **35**, 173–184.
8 Z. Xiao, S. Liao, S. Y. Rogiers, V. O. Sadras and S. D. Tyerman, *Aust. J. Graph. Wine Res.*, 2018, **24**, 487–497.
9 I. Fernandes, R. Pérez-Gregorio, S. Soares, N. Mateus and V. De Freitas, *Molecules*, 2017, **22**, 292.
10 S. Quideau, D. Deffieux, C. Douat-Casassus and L. Pouységu, *Angew. Chem., Int. Ed.*, 2011, **50**, 586–621.
11 M. N. Clifford, *J. Sci. Food Agric.*, 2000, **80**, 1063–1072.
12 O. M. Andersen and K. R. Markham, *Flavonoids: Chemistry, Biochemistry, and Applications*, CRC Press, Boca Raton, FL, 2006.
13 F. Pina, J. Oliveira and V. de Freitas, *Tetrahedron*, 2015, **71**, 3107–3114.
14 R. A. McClelland and S. Gedge, *J. Am. Chem. Soc.*, 1980, **102**, 5838–5848.
15 J. Mendoza, N. Basilio, V. de Freitas and F. Pina, *ACS Omega*, 2019, **4**, 12058–12070.
16 F. Pina, *Dyes Pigm.*, 2014, **102**, 308–314.
17 E. Echeverria, J. Burns and H. Felle, *Phytochemistry*, 1992, **31**, 4091–4095.
18 K. Yoshida, T. Kondo, Y. Okazaki and K. Katou, *Nature*, 1995, **373**, 291.
19 H. H. Felle, *Ann. Bot.*, 2005, **96**, 519–532.
20 J. A. Fenger, R. J. Robbins, T. M. Collins and O. Dangles, *Dyes Pigm.*, 2020, **178**, 11.
21 G. M. Robinson and R. Robinson, *Biochem. J.*, 1931, **25**, 1687–1705.
22 S. Asen, R. N. Stewart and K. H. Norris, *Phytochemistry*, 1972, **11**, 1139–1144.
23 T. Goto and T. Kondo, *Angew. Chem., Int. Ed. Engl.*, 1991, **30**, 17–33.
24 T. Goto, *Prog. Chem. Org. Nat. Prod.*, 1987, **52**, 113–158.
25 K. Yoshida, M. Mori and T. Kondo, *Nat. Prod. Rep.*, 2009, **26**, 884–915.
26 P. Trouillas, J. C. Sancho-García, V. De Freitas, J. Gierschner, M. Otyepka and O. Dangles, *Chem. Rev.*, 2016, **116**, 4937–4982.
27 F. He, N. N. Liang, L. Mu, Q. H. Pan, J. Wang, M. J. Reeves and C. Q. Duan, *Molecules*, 2012, **17**, 1571–1601.
28 R. Boulton, *Am. J. Enol. Vitic.*, 2001, **52**, 67–87.
29 M. Fanzone, S. Gonzalez-Manzano, J. Perez-Alonso, M. T. Escribano-Bailon, V. Jofre, M. Assof and C. Santos-Buelga, *Food Chem.*, 2015, **175**, 166–173.
30 J. A. Oliveira, J. Teixeira, N. Araujo, P. De Freitas, V. Basilio and N. Pina, *J. Agric. Food Chem.*, 2021, **69**, 1359–1367.
31 R. Brouillard, M. C. Wigand, O. Dangles and A. Cheminat, *J. Chem. Soc., Perkin Trans. 2*, 1991, 1235–1241, DOI: 10.1039/p29910001235.
32 T. Kondo, K. Yoshida, A. Nakagawa, T. Kawai, H. Tamura and T. Goto, *Nature*, 1992, **358**, 515–518.
33 J. A. Fenger, M. Moloney, R. J. Robbins, T. M. Collins and O. Dangles, *Food Funct.*, 2019, **10**, 6740–6751.
34 R. Brouillard and J. E. Dubois, *J. Am. Chem. Soc.*, 1977, **99**, 1359–1364.
35 J. Mendoza, N. Basilio, F. Pina, T. Kondo and K. Yoshida, *J. Phys. Chem. B*, 2018, **122**, 4982–4992.
36 O. Dangles, N. Saito and R. Brouillard, *J. Am. Chem. Soc.*, 1993, **115**, 3125–3132.
37 A. Mederos, S. Dominguez, E. Chinea, F. Brito, S. Midollini and A. Vacca, *Bol. Soc. Chilena Quim.*, 1997, **42**, 281–295.
38 E. A. Saad, L. H. Khalil, M. T. M. Zaki and A. A. A. El-Ella, *Microchim. Acta*, 2002, **140**, 87–91.
39 J. P. Cornard and J. C. Merlin, *J. Inorg. Biochem.*, 2002, **92**, 19–27.
40 J. P. Cornard and J. C. Merlin, *Polyhedron*, 2002, **21**, 2801–2810.
41 G. J. Smith, S. J. Thomsen, K. R. Markham, C. Andary and D. Cardon, *J. Photochem. Photobiol. A-Chem.*, 2000, **136**, 87–91.
42 J. P. Cornard, A. Caudron and J. C. Merlin, *Polyhedron*, 2006, **25**, 2215–2222.
43 S. N. Dubey and R. C. Mehrotra, *J. Inorg. Nucl. Chem.*, 1964, **26**, 1543–1550.
44 J. P. Cornard and J. C. Merlin, *J. Mol. Struct.*, 2003, **651**, 381–387.
45 A. L. Pinto, L. Cruz, V. Gomes, H. Cruz, G. Calogero, V. de Freitas, F. Pina, A. J. Parola and J. C. Lima, *Dyes Pigm.*, 2019, **170**, 7.
46 J. M. Duan and J. Gregory, *Adv. Colloid Interface Sci.*, 2003, **100**, 475–502.
47 M. C. Moncada, S. Moura, M. J. Melo, A. Roque, C. Lodeiro and F. Pina, *Inorg. Chim. Acta*, 2003, **356**, 51–61.
48 K. Yoshida, D. Ito, N. Miki and T. Kondo, *New Phytol.*, 2021, **229**, 3549–3557.
49 H. D. Schreiber, A. M. Swink and T. D. Godsey, *J. Inorg. Biochem.*, 2010, **104**, 732–739.
50 K. Yoshida, D. Ito, N. Miki and T. Kondo, *New Phytol.*, 2021, **229**, 9.
51 T. Kondo, K. Yoshida, A. Nakagawa, T. Kawai, H. Tamura and T. Goto, *Nature*, 1992, **358**, 515–518.
52 A. Nakagawa, *J. Cryst. Soc. Japan*, 1993, **35**, 327–333.
53 M. Shiono, N. Matsugaki and K. Takeda, *Proc. Jpn. Acad. Ser. B-Phys. Biol. Sci.*, 2008, **84**, 452–456.
54 F. Pina, A. Alejo-Armijo, A. Clemente, J. Mendoza, A. Seco, N. Basilio and A. J. Parola, *Int. J. Mol. Sci.*, 2021, **22**, 18.